Article

SOURCE DATA | TRANSPARENT PROCESS | OPEN ACCESS

EMBO reports

PLK1 regulates centrosome migration and spindle dynamics in male mouse meiosis

Enrique Alfaro[1], Pablo López-Jiménez[1], José González-Martínez[2], Marcos Malumbres[2], José A Suja[1] & Rocío Gómez[1,*]

Abstract

Cell division requires the regulation of karyokinesis and cytokinesis, which includes an essential role of the achromatic spindle. Although the functions of centrosomes are well characterised in somatic cells, their role during vertebrate spermatogenesis remains elusive. We have studied the dynamics of the meiotic centrosomes in male mouse during both meiotic divisions. Results show that meiotic centrosomes duplicate twice: first duplication occurs in the leptotene/zygotene transition, while the second occurs in interkinesis. The maturation of duplicated centrosomes during the early stages of prophase I and II are followed by their separation and migration to opposite poles to form bipolar spindles I and II. The study of the genetic mouse model *Plk1*(Δ/Δ) indicates a central role of Polo-like kinase 1 in pericentriolar matrix assembly, in centrosome maturation and migration, and in the formation of the bipolar spindles during spermatogenesis. In addition, *in vitro* inhibition of Polo-like kinase 1 and Aurora A in organotypic cultures of seminiferous tubules points out to a prominent role of both kinases in the regulation of the formation of meiotic bipolar spindles.

Keywords AURKA; centrosome; meiotic spindle; PCM; PLK1
Subject Categories Cell Adhesion, Polarity & Cytoskeleton; Cell Cycle
DOI 10.15252/embr.202051030 | Received 4 June 2020 | Revised 14 January 2021 | Accepted 21 January 2021 | Published online 21 February 2021
EMBO Reports (2021) 22: e51030

Introduction

Cell division requires equal segregation of the genetic material, karyokinesis, and the cytoplasmic material, cytokinesis, to both somatic daughter cells. During karyokinesis, chromosomes are driven by microtubules (MTs) to the metaphase plate and, once aligned, they are pulled towards the cell poles (Kline-Smith & Walczak, 2004). MTs are also involved in the subsequent process of cytokinesis, forming the mid-body that allows the separation of cytoplasmic material between daughter cells (Khodjakov & Rieder, 2001; Piel *et al*, 2001). MTs together with MT-organising centres (MTOCs) comprise a complex structure essential for cell division in mammals: the achromatic spindle.

Centrosomes behave as the major MTOCs in most animal cells, whereby polymerisation of MTs is implicated in cell division as well as functions such as the formation of the basal body of cilia and flagella, and the maintenance of cell shape and polarity (Azimzadeh & Marshall, 2010). Typically, centrosomes are formed by a pair of centrioles, each one composed of nine MT triplets, surrounded by an electrodense pericentriolar material (PCM). The PCM harbours not only proteins important for MT nucleation, but also regulators of the cell cycle and its checkpoints, in line with important roles for centrosomes in intracellular signalling (Woodruff *et al*, 2014). Centrioles have important roles in most microtubule-related processes, including cell motility, division and signalling. However, centrioles are not essential for MTOCs in mammalian oocytes (Dumont & Desai, 2012), nor in some insect spermatocytes (Steffen *et al*, 1986), and are absent in the first division of rodent zygotes (Coelho *et al*, 2013). Almost all land plant MTOCs also lack centrioles (Sluder, 2014). On the contrary, centrosome matrix has an evolutionarily conserved PCM protein composition (Sluder, 2014; Woodruff *et al*, 2014; Conduit *et al*, 2015).

The centrosome function is tightly coordinated with cell-cycle progression (Nigg & Holland, 2018). The centriole pair, called diplosome, undergoes a duplication during S phase, thus enabling the formation of two centrosomes that will occupy opposite poles of the dividing cell (Arbi *et al*, 2018). Duplicated centrosomes are connected by a proteinaceous link between the parental centrioles which includes centrosome-associated protein CEP250 (CEP250/CNAP1) and rootletin (Mayor *et al*, 2000). The pair of centrosomes must mature and migrate before entering mitosis in order to carry out nucleation of the spindle MTs. This maturation consists of the recruitment and accumulation of PCM proteins, such as pericentrin (PCNT; Bornens, 2012), CEP192 and CDKRAP2/CEP215, which are required for the formation of the γ-Tubulin ring complex (γTuRC; Haren *et al*, 2006). PCM reaches its maximum volume and maturation in the G2-M transition (Fujita *et al*, 2016), when γTuRC is organised around the centrosome and allows nucleation of MTs (Zheng *et al*, 1995). At the onset of mitotic cell division, duplicated centrosomes migrate to cell poles separated by the microtubule-dependent motor kinesin-like protein KIF11 (kinesin-related

1 Departamento de Biología, Facultad de Ciencias, Unidad de Biología Celular, Universidad Autónoma de Madrid, Madrid, Spain
2 Cell Division and Cancer Group, Spanish National Cancer Research Centre (CNIO), Madrid, Spain
*Corresponding author. Tel: +34 91 4978242; Fax: +34 91 4978344; E-mail: rocio.gomez@uam.es

motor protein EG5) to promote the formation of a proper bipolar spindle for karyokinesis (Blangy *et al*, 1995; Kapitein *et al*, 2005). Finally, the generation of astral MTs, which emanate from the centrosome and are connected to the cell membrane, favours the maintenance of the bipolar spindle (Kline-Smith & Walczak, 2004). Once established, the kinetochore MTs exert the driving force that allows chromosome congression and segregation. Afterwards, interzonal MTs will be responsible for executing cytokinesis (Nigg & Holland, 2018).

In 1988, Sunkel and Glover described a *Drosophila melanogaster* mutant presenting defects on cell pole establishment during cell division (Sunkel & Glover, 1988). This mutant, called *Polo*, was defective in the *Plk1* fly ortholog and allowed the description of a family of protein kinases well conserved in the evolution of eukaryotes (Vaid *et al*, 2016). Polo-like kinases are serine/threonine kinases (de Carcer *et al*, 2011). In mammals, this protein family is formed by up to five different proteins that appeared along the eukaryote evolution and present structural differences and diverse functions (Archambault & Glover, 2009). These proteins are implicated in DNA replication and repair, centrosome duplication and maturation; and cell division regulation and cytokinesis (Schmucker & Sumara, 2014).

In mitosis, kinases CDK1 and Aurora A (AURKA) are essential for Polo-like kinase 1 (PLK1) regulation (Lukasiewicz & Lingle, 2009; Nikonova *et al*, 2013). The location, activation and function of PLK1 are highly regulated, and defects on these processes are involved in the appearance of aneuploidies and carcinogenesis (Liu *et al*, 2017). The PLK1 protein has three domains, a catalytic N-terminal domain, a C-terminal Polo-box type domain and a binding domain of these two previous ones (de Carcer *et al*, 2011). The N-terminal domain corresponds to its active site, involved in its kinase function, and in the regulation of its activation loop; the Polo-box domain in turn participates in ligand recognition (Schmucker & Sumara, 2014). Residues serine 137 (S137) and threonine 210 (T210) are located in the activation loop, and their phosphorylation is essential for the regulation of PLK1 (Tsvetkov & Stern, 2005).

During mitosis, PLK1 participates in centrosome maturation and the establishment of the spindle (Zitouni *et al*, 2014), as well as cohesin complex removal (Hauf *et al*, 2005) and cytokinesis (Fabbro *et al*, 2005). Mitotic PLK1 is localised at centrosomes, kinetochores and mid-body (Barr *et al*, 2004). The dissolution of the link between duplicated centrioles at the onset of mitosis, a process termed centrosome separation, is dependent on PLK1 and AURKA kinases (Fujita *et al*, 2016). Once the duplicated centrosomes have separated, their migration towards the cell poles can occur mediated by kinesin KIF11, which is also regulated by PLK1 and CDK1 (Agircan *et al*, 2014).

Although there is great knowledge about the functional role of PLK1 during mitosis, much less is known about its importance during meiosis, the special cell division process that allows the formation of haploid gametes. Meiosis implies two rounds of chromosome segregation after a single round of DNA replication. During the first meiotic division, chromosomes undergo a process of DNA exchange called recombination, which provides genetic diversity to the resulting gametes (Miller *et al*, 2013). In prophase I, homologous chromosomes pair, synapse, recombine and desynapse in a coordinated process that requires the formation of a tripartite protein structure called the synaptonemal complex (SC; Page & Hawley, 2004; Hunter, 2015), followed by the reductional segregation of recombined homologous chromosomes during anaphase I. During the second meiotic division, sister chromatids segregate in anaphase II in an equational manner to allow the formation of haploid gametes. Several important roles for PLK1 have been described in mammalian oogenesis, where progression is arrested during prophase I at the stage of dictyotene. PLK1 is needed for the resumption of cell division before ovulation (Hunt & Hassold, 2002), and for the establishment of the female acentriolar meiotic spindle, localising to the MTOCs (Xiong *et al*, 2008). In addition, PLK1 carries out specific functions such as nuclear envelope breakdown (NEBD), and activation of the anaphase promoting complex and chromosome condensation maintenance (Solc *et al*, 2015). Nevertheless, knowledge about the extended roles of PLK1 in vertebrate spermatogenesis is considerably limited.

This work is focused on addressing the role of PLK1 and AURKA in centrosome regulation and in the establishment of male mouse meiotic spindles. Mammalian male meiotic centrosomes present centrioles and act as MTOCs. These centrioles are needed for the formation of spermatozoa flagellum and, in many mammals including human, are inherited by the zygote to constitute the first centrioles of an organism (Coelho *et al*, 2013). Therefore, correct MTOC and spindle formation and regulation in meiosis are essential for male fertility.

Results

Centrosome migration starts at the diplotene and prophase II stages

In order to learn about male mouse meiotic centrosomes, we have studied its composition and dynamics on squashed spermatocytes since this technique does not disturb the tridimensionality of cell morphology, neither chromosome condensation and protein distribution in prophase I and dividing spermatocytes (Page *et al*, 1998).

We first determined the distribution of PCM components. For this, we performed a double immunofluorescence staining of PCNT, the major structural protein of PCM (Delaval & Doxsey, 2010), together with SYCP3, a component of the SC commonly used as marker of meiosis progression (Parra *et al*, 2004). In early prophase I (leptotene and zygotene), a small and round PCNT signal appears externally but highly proximal to the nucleus. In these stages, SYCP3, a component of the SC, marked the newly formed axial elements (AEs) and lateral elements (LEs) in those places where synapses have already been established between the homologues (Fig 1A). In pachytene, a large and diffuse PCNT signal is observed, while SYCP3 marks the fully synapsed autosomal chromosome LEs and the AEs and the pseudoautosomal region of the XY sex pair (Fig 1B). In diplotene, SYCP3 marks the desynapsed LEs, and two compact signals of PCNT are clearly distinguished. These signals are comparatively smaller and more compact than the pachytene signal and can be observed very close to each other. This result suggests that both signals correspond to the two centrosomes, which are already identified separately (Fig 1C), indicating the onset of the separation of the centrosomes. At diakinesis, PCNT foci begin to separate, although they remain very close to the nuclear periphery. At this stage, SYCP3 marks synapsed and desynapsed LEs and small

cytoplasmic agglomerations (Fig 1D), in accordance with previous results (Parra *et al*, 2004). In prometaphase I, two intense PCNT signals are oriented towards the poles of the cell, although bivalents are not yet fully aligned (Fig 1E). In metaphase I, two PCNT signals are located at the opposite poles of the cell (Fig 1F). SYCP3 labels the inner centromeric domain and the interchromatid domain (Fig 1E and F). In telophase I, two groups of PCNT signals are observed, one at each pole, in which several small PCNT foci can be observed. SYCP3 is observed as small bars on segregated homologous chromosomes (Fig 1G).

In interkinesis, SYCP3 is presented as bars and PCNT conforms two small foci very close to each other (Fig 2A). During the second meiotic division, at early prophase II, two small signals of PCNT are still observed (Fig 2B). Following this stage, SYCP3 is no longer detected, as previously described (Parra *et al*, 2004). It is in late prophase II that the two signals of PCNT begin to distance themselves (Fig 2C). In prometaphase II, two signals of PCNT are already oriented towards the opposite poles of the cell and close to the chromosomes (Fig 2D). In metaphase II, chromosomes are aligned, and PCNT signals are observed in each pole (Fig 2E). In telophase II, we observe a PCNT signal in each pole of the cell along with the two daughter nuclei (Fig 2F).

Centrosomes duplicate twice during male mouse meiosis

We then focused on analysing the timing of centrosome duplication during meiosis. To do this, we immunolabelled a structural component of centrioles with anti-Centrin-3 antibody together with SYCP3. In early prophase I, Centrin-3 (CETN3) is detected as two small and very proximal dots near the nucleus in leptotene (Fig 3A and A′), while it clearly shows four small signals, two pairs, in zygotene (Fig 3B and B′) and pachytene (Fig 3C and C′). This suggests that centrosome duplication occurs in the transition from leptotene to zygotene. Centrioles are always seen near the nucleus; however, as the result of z-projection, some centrioles appear immersed in DAPI signals in the images. CETN3 is clearly seen as two dots per opposite poles in metaphase I (Fig 3D and D'). When bivalents are segregated in telophase I, two CETN3 dots are visible in each pole (Fig 3E and E′). In early interkinesis, two small signals of CETN3 are detected (Fig 3F and F') and four dots are clearly seen in late interkinesis (Fig 3G and G'). This suggests a second centrosome duplication between the first and the second meiotic divisions. The newly duplicated centrosomes start separating again in prophase II (Fig 3H and H'). Two clear signals of CETN3 at the poles are also visible in metaphase II (Fig 3I and I′) and in telophase II (Fig 3J and

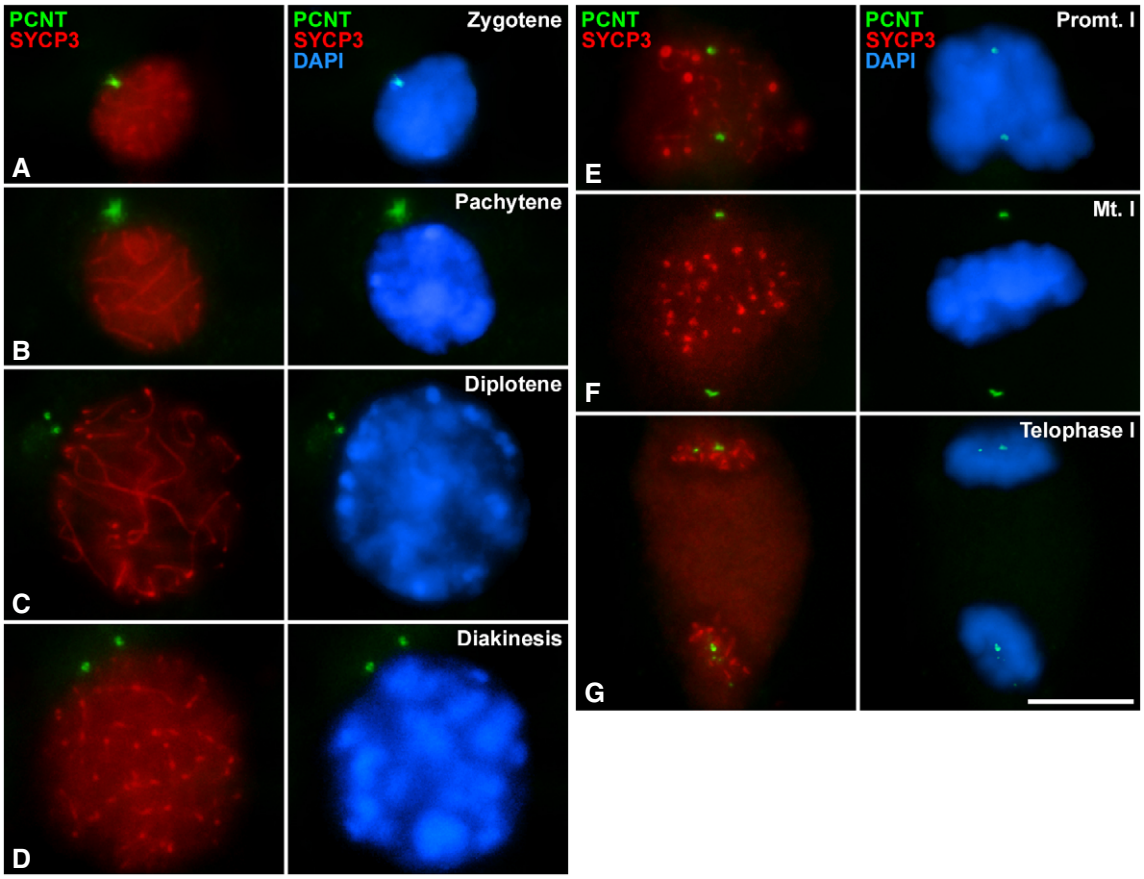

Figure 1. Distribution of PCNT and SYCP3 during the first meiotic division.

A–G Double immunolabelling of pericentrin -PCNT- (green) and SYCP3 (red) on squashed WT mouse spermatocytes on (A) zygotene, (B) pachytene, (C) diplotene, (D) diakinesis, (E) prometaphase I, (F) metaphase I and (G) telophase I. Chromatin has been stained with DAPI (blue). Scale bar in G represents 10 μm.

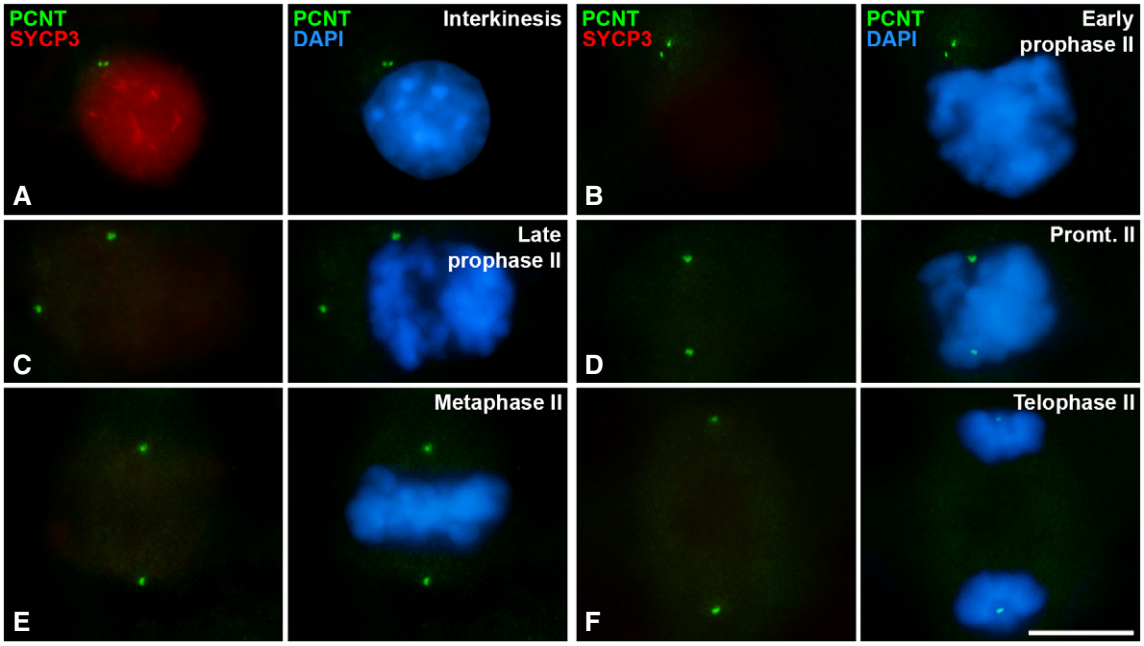

Figure 2. Distribution of PCNT and SYCP3 during interkinesis and the second meiotic division.

A–F Double immunolabelling of pericentrin -PCNT- (green) and SYCP3 (red) on squashed WT mouse spermatocytes at (A) interkinesis, (B) early prophase II, (C) late prophase II, (D) prometaphase II, (E) metaphase II and (F) telophase II. Chromatin has been stained with DAPI (blue). Scale bar in F represents 10 μm.

J′). Spermatids show a pair of centrioles in early (Fig 3K and K′) and late (Fig 3L and L′) maturation stages. These results indicate that centrosomes duplicate twice during male mouse meiosis: in leptotene-zygotene transition and during interkinesis.

To further confirm these results, a double immunolabelling of γ-Tubulin, a centrosome marker, together with SYCP3 was analysed in both meiotic divisions (Fig EV1). γ-Tubulin was appreciated as a single round mark in pachytene (Fig EV1A), while it appeared as two signals when centrosomes migrated in diplotene and diakinesis (Fig EV1B and C). γ-Tubulin is detected at the bipolar spindles at the first (Fig EV1D) and second (Fig EV1F) meiotic divisions. Two signals of γ-Tubulin are also detected in late interkinesis (Fig EV1A). All data of γ-Tubulin are in accordance with PCNT and CETN3 patterns of localisation (Figs 1–3).

Genetic depletion of *Plk1* indicates a role of PLK1 in PCM assembly and in the regulation of centrosome migration

In order to verify the localisation of PLK1 at the centrosomes in male mouse meiosis, we first detected its phosphorylated modification PLK1S137P in squashed spermatocytes, since it was previously described in mouse oocytes (Du *et al*, 2015). In pachytene, PLK1S137P diffusely decorated the nucleoplasm, showing intense signals at the chromocentres, which represent clustered centromeres (Fig 4A). In addition, two signals are detected near to the nucleus. These signals colocalise with γ-Tubulin (Fig 4B), indicating the position of the centrosome. In late diplotene, PLK1S137P signals are slightly separated from each other (Fig 4C) at the onset of centrosome migration. In diakinesis, separated signals are clearly detected (Fig 4E). This same separation is observed with γ-Tubulin (Fig 4D and F). When bivalents are aligned in the metaphase I plate, intense PLK1S137P and γ-Tubulin signals at the centrosomes are clearly located at opposite poles. In addition, centromeric signals of PLK1S137P are detected (Fig 4G and H). The same pattern is observed during the second meiotic division, with a second centrosome migration during prophase II and the location of PLK1S137P and γ-Tubulin in opposite poles at metaphase II (Fig 4I and J). The PLK1S137P pattern of distribution was also confirmed in spread spermatocytes (Fig EV2E–J). Distribution of PLK1T210P, another modification of PLK1 (Du *et al*, 2015), was also studied in squashed (Fig EV2A and B) and spread spermatocytes (Fig EV2C and D); however, no centrosomic signals were detected with this modification.

We then performed a genetic approach examining *Plk1*-deficient mice generated previously (Wachowicz *et al*, 2016; de Carcer *et al*, 2017), whose meiotic phenotype has not yet been described. Since constitutive knock-out alleles for each gene are lethal in homozygosis, we used male mice carrying conditional knock-out (cKO) alleles in combination with a Cre recombinase allele that can be induced by tamoxifen (TX) (Fig EV3). We analysed the centrosome dynamics in *Plk1*(lox/lox) mice after a 7 day of TX treatment, *Plk1*(Δ/Δ), since the health of the mice deteriorated critically leading to death after this period (Wachowicz *et al*, 2016; de Carcer *et al*, 2017). These *Plk1*(Δ/Δ) mice reduce 86% *Plk1* levels in testis (Wachowicz *et al*, 2016). Gene strategy from Wachowicz *et al*. is displayed in Fig EV3 A. Efficient excision of the corresponding targeted exon in testis from TX-treated *Plk1*(Δ/Δ) mice was confirmed by PCR (Fig EV3B). Immunofluorescence signals for PLK1 at centrosomes in *Plk1*(Δ/Δ) metaphases presented levels below the detection threshold, while CETN3 confirmed the position of centrosomes.

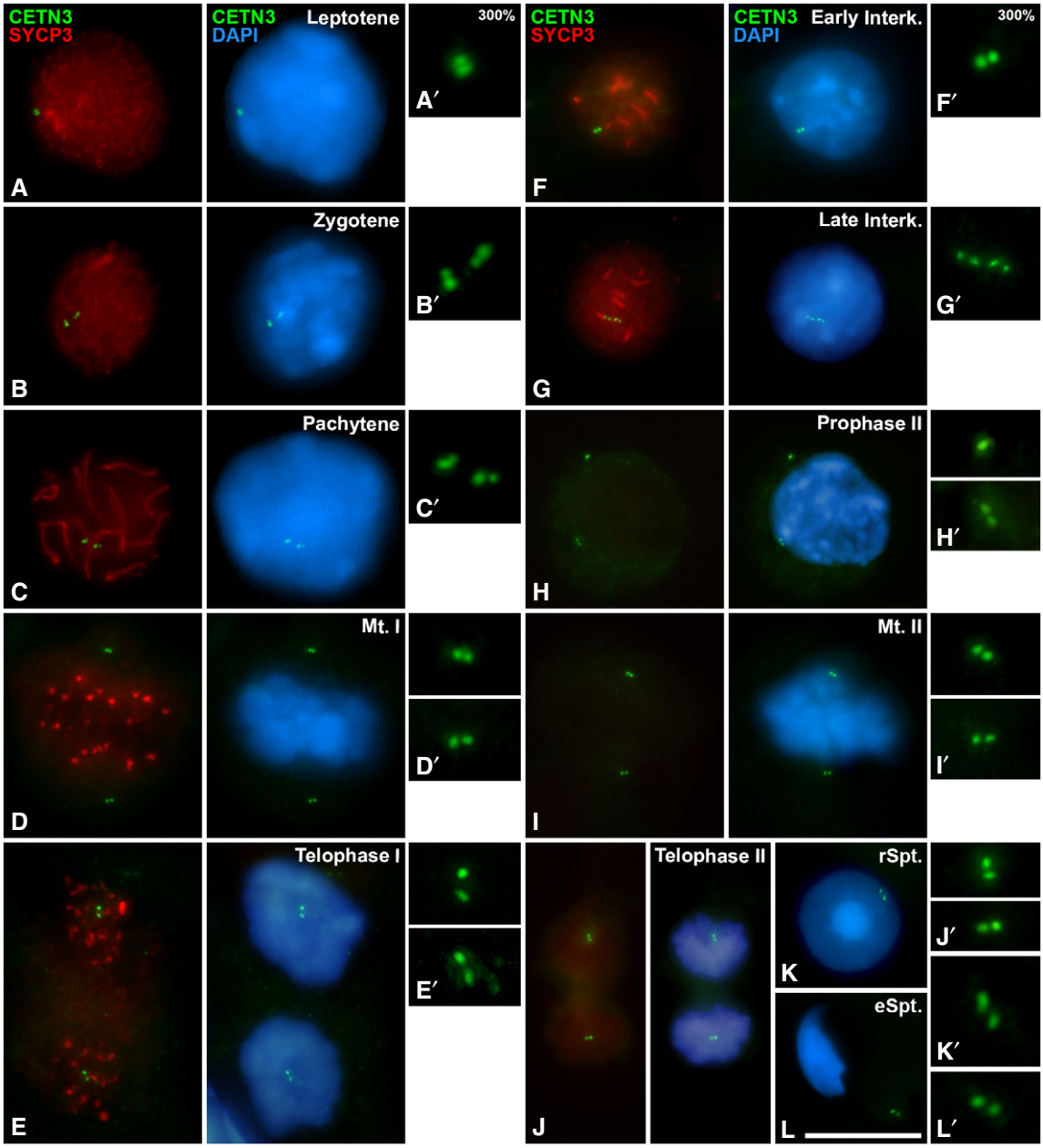

Figure 3. Distribution of CETN3 and SYCP3 during spermatogenesis.

A–L Double immunolabelling of CETN3 (green) and SYCP3 (red) on squashed WT mouse spermatocytes at (A) leptotene, (B) zygotene, (C) pachytene, (D) metaphase I, (E) telophase I, (F) early interkinesis (F), late interkinesis (G), prophase II (H), metaphase II (I), telophase II (J), round spermatid (K) and elongated spermatid (L). Amplifications at 300% magnification for the centrosomic CETN3 signals are presented for each image. Chromatin has been stained with DAPI (blue). Scale bar in L represents 10 μm.

Quantification analysis offers significance in comparison to control metaphases (Fig EV3C). Although mice were not able to survive longer periods of *Plk1* ablation, having proliferative tissue seriously affected, the histological sections of *Plk1*(Δ/Δ) seminiferous tubules showed minimal apoptosis (Fig EV3D). The level of apoptosis detected by immunolabelling cleaved caspase-3 (caspase-3) showed no significant differences between *Plk1*(+/+) and *Plk1*(Δ/Δ) mice (Fig EV4F). Altogether, these data suggest that somatic division in proliferative tissues severely alters the animal's health (Wachowicz *et al*, 2016; de Carcer *et al*, 2017), yet *Plk*1 ablation can be studied in testis.

Plk1(+/+) mice (onwards control) present centrosomes that duplicate in the transition from leptotene to zygotene (Fig 5A and A'), are already duplicated in pachytene (Fig 5B and B') and start migrating in diplotene (Fig 5C and C'). The separation between centrosomes is detected with PCNT and CETN3 in diakinesis

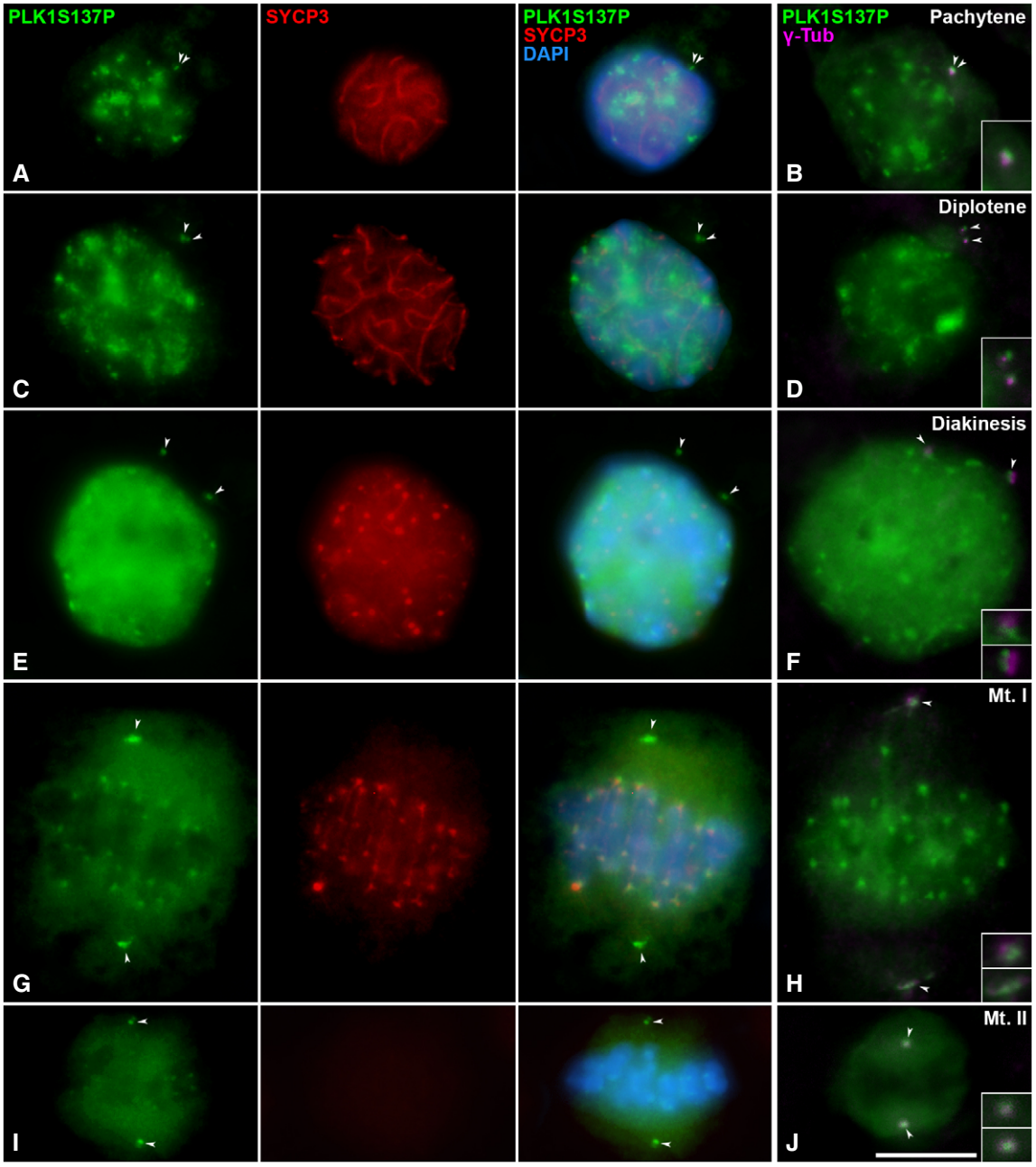

Figure 4. PLK1S137P distribution during male mouse meiosis.

A–J Double immunolabelling of PLK1S137P (green) and SYCP3 (red) on squashed WT mouse spermatocytes at (A) pachytene, (C) diplotene, (E) diakinesis, (G) metaphase I and (I) metaphase II. Chromatin has been stained with DAPI (blue). Fourth column shows the double immunolabelling of PLK1-S137P (green) and γ-Tubulin (magenta) on squashed WT mouse spermatocytes at (B) pachytene, (D) diplotene, (F) diakinesis, (H) metaphase I and (J) metaphase II. Insets correspond to centrosomes at 200% magnification. White arrows indicate the location of centrosomes. Scale bar in J represents 10 μm.

(Fig 5D and D'). All signals of CETN3 are embedded in a PCM containing PCNT in control prophase I spermatocytes (Fig 5A–D; A'–D'), and the absence of PCNT signal is never observed in control prophase I cells. In contrast, in early prophase I *Plk1*(Δ/Δ) cells, an absence of PCNT signals was observed in 14.25% of zygotene cells and 14.5% of pachytene cells (Fig 5E and F). Quantification of the absence of PCNT (PCNT- cells) has been done for zygotene (Fig 5M), pachytene (Fig 5N) and diplotene (Fig 5O) stages of control and *Plk1*(Δ/Δ) spermatocytes. In these cells, the triple immunolabelling of CETN3, PCNT and SYCP3 accurately verifies the location of centrioles in the absence of PCNT (Fig 5E–F; E'–F'). Cells in diplotene present adjacent centrosomes that would be presumably unable to migrate in the absence of PLK1 activity (Fig 5G and G'). In accordance, *Plk1*(Δ/Δ) diakinesis presented

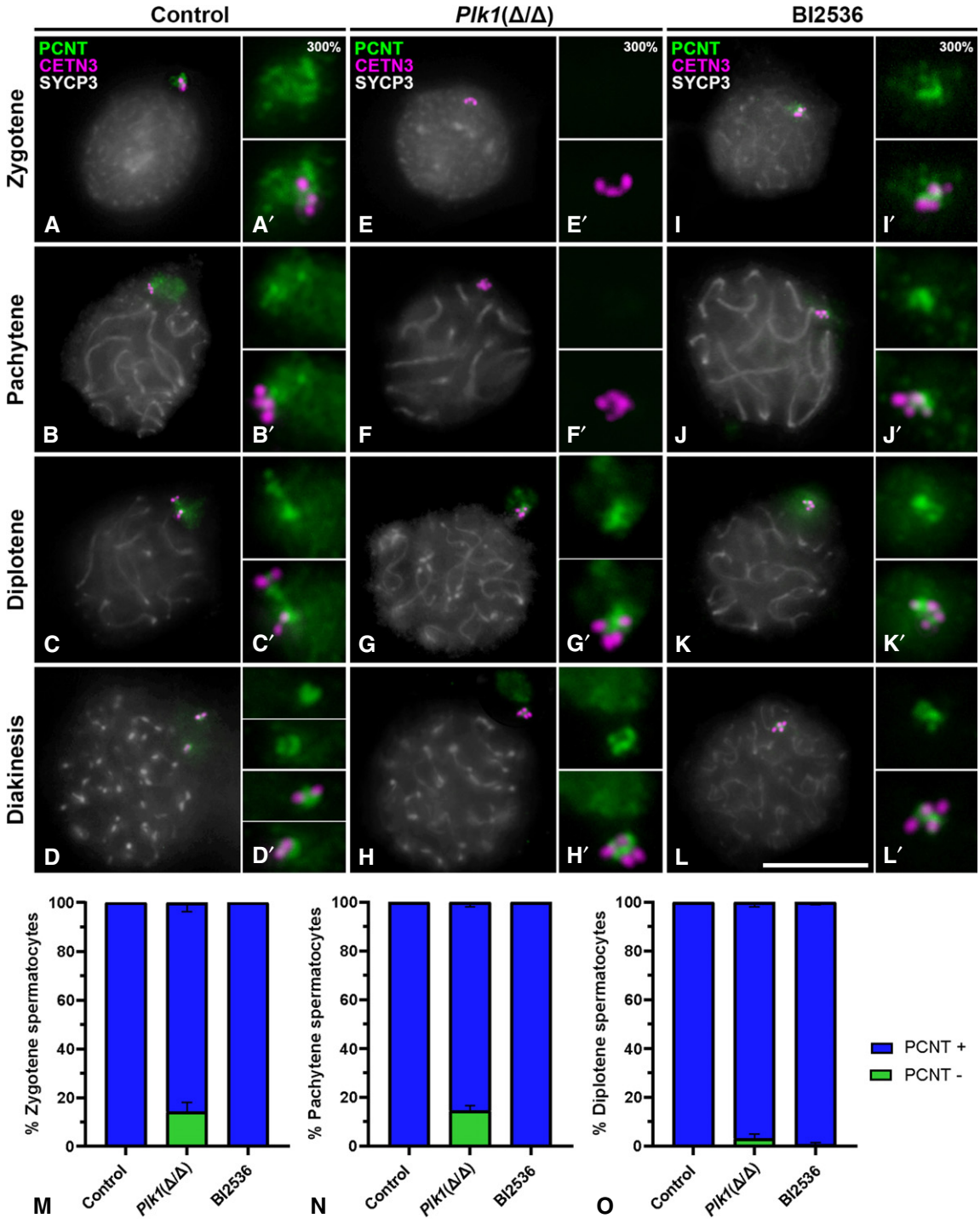

Figure 5. Triple immunolabelling of PCNT, CETN3 and SYCP3 during prophase I in control, *Plk1*(Δ/Δ) and BI2536-treated spermatocytes†.

A–L First column shows the triple immunolabelling of CETN3 (green), PCNT (red) and SYCP3 (grey) on squashed WT mouse spermatocytes. Second column shows the correspondent labellings for *Plk1*(Δ/Δ). Third column shows signals for BI2536-treated spermatocytes. Images are shown for (A, E, I) zygotene, (B, F, J) pachytene, (C, G, K) diplotene and (D, H, L) diakinesis. Amplifications at 300% magnification for all labellings are displayed for each image.

M–O Quantification of the percentage of cells without PCNT at centrosomes (PCNT-) in (M) zygotene, (N) pachytene and (O) diplotene in control, *Plk1*(Δ/Δ) and BI2536-treated spermatocytes. Data for BI2536 represent results for 100 μM at 8-h treatment on organotypic cultures of seminiferous tubules. Data are presented as mean ± SD for three biological replicates for each condition.

Data information: Scale bar in L represents 10 μm.
Source data are available online for this figure.
†Correction added on 10th March, after first online publication: The contrast of panels A-L was decreased.

adjacent centrosomes after their arrest of migration in the previous diplotene stage (Fig 5G and H). In diplotene and diakinesis, four proximal CETN3 signals seem to be enclosed in one single PCM in non-migrated centrosomes (Fig 5G and H). Therefore, these results suggest a role of PLK1 in PCM assembly and in the regulation of meiotic centrosome migration.

BI2536 impairs centrosome migration in prophase I

After studying the phenotype of *Plk1*(Δ/Δ) prophase I spermatocytes, we then analysed the role of PLK1 with a functional study *in vitro* using the pharmacological inhibitor BI2536 (Steegmaier *et al*, 2007), which inhibits PLK1 in somatic cells (Lenart *et al*, 2007), mouse spermatocytes (Jordan *et al*, 2012) and mouse oocytes (Du *et al*, 2015). We treated organotypic cultures of seminiferous tubules with 100 μM BI2536 for 8 h, a higher concentration that previously reported for cell suspensions (Jordan *et al*, 2012). Exhaustive analysis of the optimisation of this protocol is displayed in Fig EV4. The employed concentration and treatment duration did not alter cell viability, as the level of apoptosis detected by immunolabelling caspase 3 showed no significant differences between the control spermatocytes versus the BI2536-treated ones (Fig EV4A–F). At least 8-h BI2536 treatment was necessary to observe morphological alterations, monopolar spindles (Fig EV4D–E), and longer culture periods were discarded as control cultures severely compromise cell viability after 24 h (Fig EV4C). Therefore, the *in vitro* treatment with BI2536 in organotypic cultures of seminiferous tubules is not directly related to an increase in apoptosis in our experimental conditions. Following this methodological approach, we compared prophase I spermatocytes from control, *Plk1*(Δ/Δ) and BI2536-treated spermatocytes during prophase I.

In vitro inhibition of PLK1 with BI2536 during 8 h is not long enough to progress preleptotene cells into leptotene/zygotene under BI2536 effect, according to the fact that spermatocytes take several days to progress between spermatogonia to pachytene (Griswold, 2016; Romer *et al*, 2018; Enguita-Marruedo *et al*, 2019). Under these circumstances, we observed during zygotene the presence of PCNT at centrosomes (Fig 5I, I' and M). PCNT also persisted at pachytene stage (Fig 5J and J'). Adjacent non-migrated centrosomes are observed in BI2536-treated diplotene and diakinesis spermatocytes, as a clear effect of impairment of centrosome migration under BI2536 treatment (Fig 5K, K' and L, L'). In these stages, four proximal CETN3 signals indicate an arrest of the centrosome migration, assuming that both centrosomes seem to be enclosed in one single PCM (Fig 5K and L). Quantification of the absence of PCNT (PCNT- cells) has also been done for BI2536-treated spermatocytes in zygotene (Fig 5M), pachytene (Fig 5N) and diplotene (Fig 5O). Taken together, these data indicate that centrosome migration is inhibited in prophase I after BI2536 *in vitro* treatment, in accordance with the *Plk1*(Δ/Δ) mouse model results.

Absence of PCNT impairs γ-Tubulin recruitment to centrosomes in *Plk1*(Δ/Δ)

Double immunolabellings of PCNT with SYCP3 or PCNT with γ-Tubulin were performed in order to ascertain the presence of γTuRC in centrosomes at the different experimental conditions. The γ-Tubulin signals are embedded in PCNT-containing PCMs at all control prophase I stages (Fig 6A). In contrast, γ-Tubulin is not detected at pachytene when PCNT has not been recruited to *Plk1* (Δ/Δ) centrosomes (Fig 6B a–b). γ-Tubulin was detected partially colocalising with PCNT in non-migrated centrosomes of *Plk1*(Δ/Δ) at diplotene and diakinesis stages (Fig 6B c–f). On the other hand, these results were not appreciated in BI2536 as an 8-h treatment is not long enough to induce alteration in PCM assembly from premeiotic stages to pachytene, in correlation with Fig 5. Nevertheless, BI2536 8-h treatment showed aberrant excrecencies in PCNT appearance in cells at pachytene and arrested centrosome migration in diplotene and diakinesis stages (Fig 6C).

To further confirm these results, γ-Tubulin was labelled together with CETN3. γ-Tubulin and CETN3 are located at centrosomes in control pachytene spermatocytes, while the presence of CETN3 confirms the presence of centrioles in *Plk1*(Δ/Δ) pachytenes that have not recruited γ-Tubulin to centrosomes (Fig 6D a–b). Migrated centrosomes are seen in control diakinesis, while non-migrated centrosomes are visible in *Plk1*(Δ/Δ) (Fig 6D c–d). Altogether, these results suggest that a PLK1-regulated presence of PCNT at meiotic centrosomes is essential for the location of γ-Tubulin. Quantification of the number of spermatocytes in pachytene and diplotene in *Plk1* (Δ/Δ) and BI2536-treated cultures is presented in Fig 6E.

PLK1 and AURKA kinases regulate the formation of bipolar meiotic spindles I and II

When bivalents are aligned at the metaphase I plate, centrosomes have completed their migration towards opposite poles in control spermatocytes, and bipolar spindles are unambiguously observed. In these spermatocytes, SYCP3 appears as intense centromeric signals and faint interchromatid domain patches (Parra *et al*, 2004), and kinetochore MTs reach the aligned bivalents at the metaphase I plate (Fig 7A). Aligned bipolar spindles II are observed in control metaphase II (Fig 7B). PCNT is detected at the opposite poles in these bipolar spindles (Fig 7C and D). In contrast, *Plk1*(Δ/Δ) presented cells with non-migrated poles with a level of chromatin condensation corresponding to prometaphase I/metaphase I and prometaphase II/metaphase II, respectively. We will classify these cells as monopolar spindles I (Fig 7E) and monopolar spindles II (Fig 7F). *Plk1*(Δ/Δ) monopolar spindles I and II show two PCNT signals very proximal to each other, corroborating a single pole per cell (Fig 7G and H). The known target of PLK1, centromere protein U (CENP-U) (Kang *et al*, 2011), is not detected in its phosphorylated form (CENP-UP) in *Plk1*(Δ/Δ) monopolar spindles (Fig EV5B), in contrast to control (Fig EV5A). In these monopolar spindles I and II, bivalents and chromosomes, respectively, are not located to form a correct metaphase plate but arranged into an irregular crown around the MTs emanating from the monopolar spindle. Testis cryosections counterstained with DAPI also showed dividing spermatocytes in a crown arrangement that seem to correspond to monopolar metaphases (Fig EV3C). The squashing technique allowed us to verify in a three-dimensional view the control bipolar spindles I (Movie EV1) versus *Plk1*(Δ/Δ) monopolar spindles I (Movie EV2).

When spermatocytes are cultured *in vitro*, BI2536 impairs the formation of bipolar spindles I and II (Fig 7I and J), indicating that the *ex vivo* inhibition of PLK1 shows correlation with the phenotype of the genetic model *Plk1*(Δ/Δ). In BI2536 monopolar spindles, PCNT is detected as two clear signals in the same pole, from which

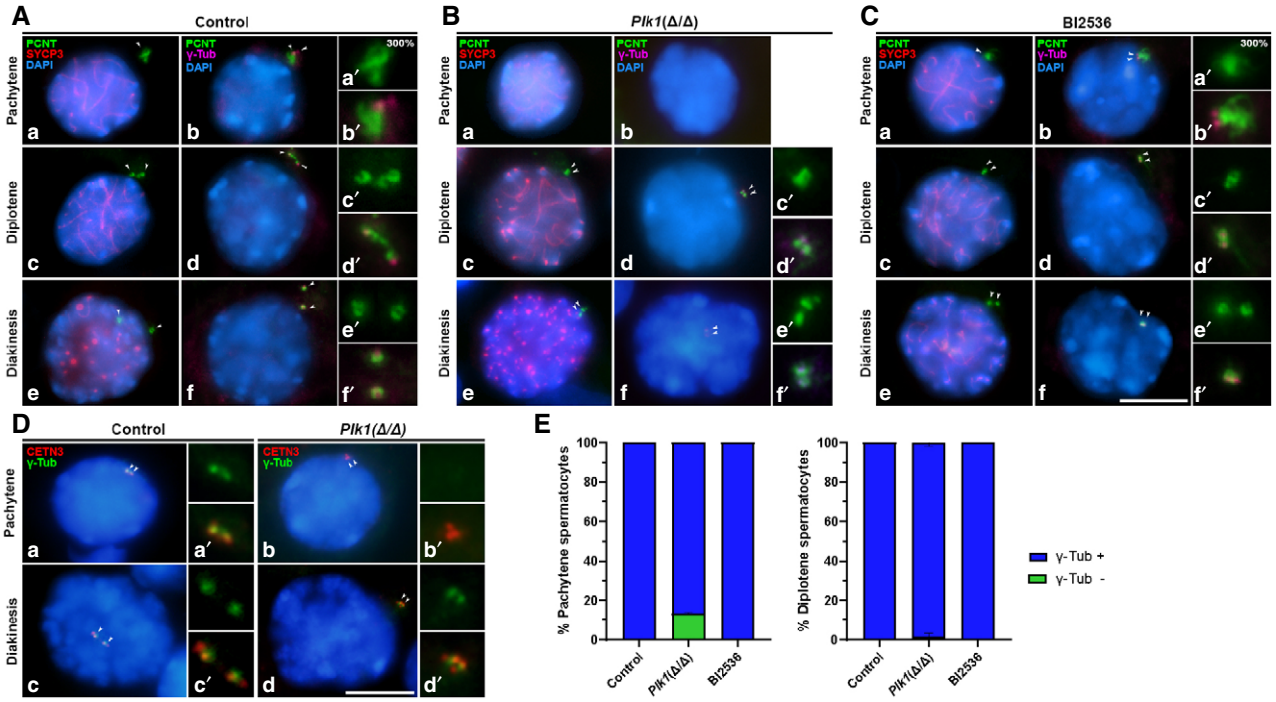

Figure 6. Immunolabelling of γ-Tubulin and SYCP3 and CETN3 and γ-Tubulin.

A–C Immunolabelling of γ-Tubulin and SYCP3 during prophase I in control, *Plk1*(Δ/Δ) and BI2536-treated spermatocytes. Images are shown for pachytene, diplotene and diakinesis in Control (A), *Plk1*(Δ/Δ) (B) and BI2536-treated spermatocytes (C). First columns show the double immunolabelling of PCNT (green) and SYCP3 (red), and second columns shows γ-Tubulin (γ-Tub, magenta) and SYCP3 (red). Chromatin has been stained with DAPI (blue). Amplifications at 300% magnification for all labellings are displayed for each image. Data for BI2536 represent results for 8 h at 100 μM treatment on organotypic cultures of seminiferous tubules.

D Immunolabelling of CETN3 and γ-Tubulin in control and *Plk1*(Δ/Δ). Double immunolabelling of CETN3 (red) and γ-Tubulin (green) in pachytene (a, b) and diakinesis (c, d). Chromatin has been stained with DAPI (blue).

E Quantification of the number of cells without γ-Tubulin at centrosomes (γ-Tub -) in pachytene and diplotene spermatocytes in control, *Plk1*(Δ/Δ) and BI2536-treated spermatocytes. Data represent average of two biological replicates per condition. Data are mean ± SD.

Data information: White arrows indicate the location of centrosomes. Scale bar in C–f and D–d represents 10 μm.
Source data are available online for this figure.

the MTs detected with α-Tubulin emanated (Fig 7K and L). We also tested the efficiency of BI2536 by detecting CENP-UP, which is absent at the pole of monopolar spindles (Fig EV5C).

Given the known role of AURKA, localised at centrosomes, in the regulation of mitotic (Tang *et al*, 2017) and oocyte (Saskova *et al*, 2008) spindle formation, we then selectively inhibited this kinase using MLN8237 at 10 μM in cultured seminiferous tubules. This drug, also called Alisertib, is extensively used in somatic cells (Kollareddy *et al*, 2012) and has also been used in oogenesis research (Nguyen *et al*, 2018). Optimisation of this protocol for spermatocytes is shown in Fig EV4. This approach showed that the *in vitro* inhibition of AURKA with MLN8237 also impaired the formation of bipolar spindles I and II in mouse spermatogenesis (Fig 7M and N). PCNT is also detected at the single pole in monopolar MLN8237 spindles I and II (Fig 7O and P). However, MLN8237 treatment did not alter CENP-UP signal, which is detected at kinetochores and centrosomes (Fig EV5D). MLN8237 monopolar spindles I and II also showed a crown MT arrangement, equally to BI2536 and *Plk1*(Δ/Δ) monopolar spindles.

The appearance of monopolar spindles I and II in *Plk1*(Δ/Δ), BI2536-treated and MLN8237-treated spermatocytes was statistically significative in comparison to control (Fig 7Q and R) for both meiotic divisions. These results indicate that PLK1 and AURKA functions are important for the accurate formation of meiotic spindles I and II.

Depletion or inhibition of PLK1 alters the pattern of AURK phosphorylation at meiotic centrosomes

After studying the consequences of *Plk1* ablation in *Plk1*(Δ/Δ) and observing the effects of PLK1 *in vitro* inhibition with BI2536, plus analysing the inhibition of AURKA with MLN8237, we wondered if PLK1 disruption has an effect on AURK pattern of distribution or phosphorylation. AURKA belongs to a family of three kinases with high sequence homology (Nguyen & Schindler, 2017; Tang *et al*, 2017). Therefore, we used an antibody that detects these three kinases in their phosphorylated form: phosphorylated Aurora kinases (AURKP) (Nguyen & Schindler, 2017). AURKP antibody detects centromeric signals that correspond to phosphorylated AURKB/C (AURKB/CP), and a clear pattern at the centrosomes, corresponding to phosphorylated AURKA (AURKAP) (Tang *et al*, 2017). With the use of this antibody, we could distinguish

differences in the pattern of distribution of the three phosphorylated kinases in the same cell. Our results showed that control metaphases I and II present a clear signal of AURKP at the poles of the bipolar spindles, detected by α-Tubulin, that corresponds to AURKAP. In addition, strong centromeric signals are visible, presumably corresponding to AURKB/CP (Fig 8A a and b). No monopolar spindles are seen in control. AURKAP is detected at centrosomes of bipolar spindles found in *Plk1*(Δ/Δ) spermatocytes (Fig 8A c and d). By contrast, *Plk1*(Δ/Δ) monopolar spindles I and II showed absent or significantly reduced signals of AURKP at the centrosomes, although centromeric signals are still observed, yet slightly less compact (Fig 8B a and b). Accordingly, bipolar spindles found in BI2536-treated cultures showed AURKP at the centrosomes (Fig 8A e and f), but monopolar spindles I and II showed absent or significantly reduced signals of AURKP at the poles (Fig 8B c and d). In addition, we corroborated the inhibition of AURKA with MLN8237, where AURKP is absent at centrosomes both in bipolar and monopolar spindles of cultures treated with this drug (Fig 8A g and h; Fig 8B e and f). Data quantification for the percentage of cells lacking AURKP at poles (AURKAP) is represented in graphs for

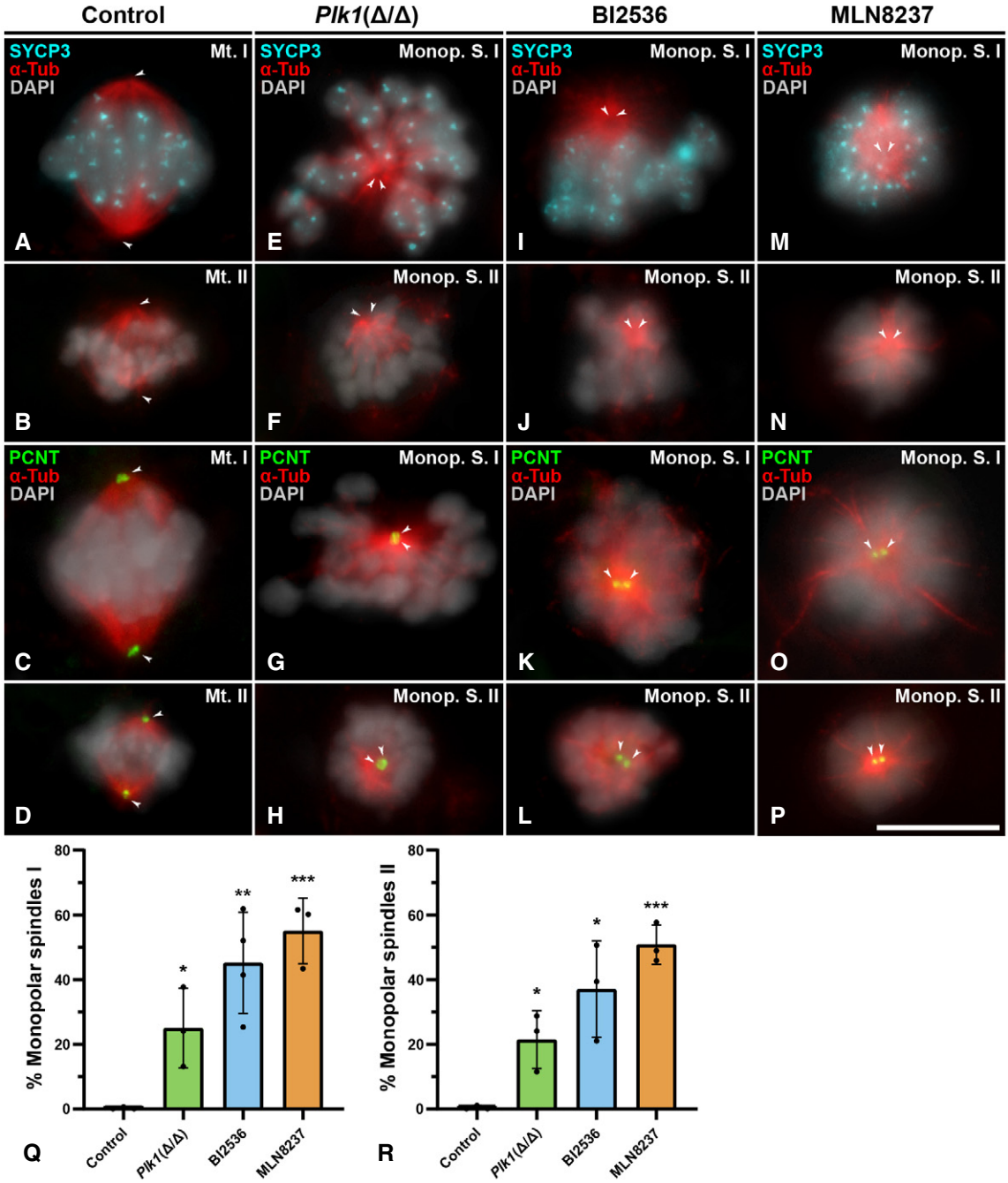

Figure 7.

Figure 7. Meiotic spindles I and II in control, *Plk1*(Δ/Δ), BI2536-treated and MLN8237-treated spermatocytes.

A–D Control: Double immunolabelling of SYCP3 (cyan) and α-Tubulin (red) on control squashed spermatocytes for the first and the second meiotic divisions at metaphase I (A) and metaphase II (B). Double immunolabelling of PCNT (green) and α-Tubulin (red) on control squashed spermatocytes at metaphase I (C) and metaphase II (D). Chromatin has been stained with DAPI (pseudocoloured in grey).

E–H *Plk1*(Δ/Δ) mouse model: Double immunolabelling of SYCP3 (cyan) and α-Tubulin (red) in monopolar spindle I (E) and monopolar spindle II (F). Double immunolabelling of PCNT (green) and α-Tubulin (red) labelling in monopolar spindle I (G) and monopolar spindle II (H). Chromatin has been stained with DAPI (pseudocoloured in grey).

I–L BI2536-treated spermatocytes: Double immunolabelling of SYCP3 (cyan) and α-Tubulin (red) at monopolar spindle I (I) and monopolar spindle II (J). Double immunolabelling of PCNT (green) and α-Tubulin (red) labelling in monopolar spindle I (K) and monopolar spindle II (L). Chromatin has been stained with DAPI (pseudocoloured in grey). Cells shown were treated for 100 μM BI2536 for 8-h treatment on organotypic cultures of seminiferous tubules.

M–P MLN8237-treated spermatocytes: Double immunolabelling of PCNT (green) and α-Tubulin (red) in monopolar spindle I (M) and monopolar spindle II (N). Double immunolabelling of PCNT (green) and α-Tubulin (red) in monopolar spindle I (O) and monopolar spindle II (P). Chromatin has been stained with DAPI (pseudocoloured in grey). Cells shown were treated for 10 μM MLN8237 for 8-h treatment on organotypic cultures of seminiferous tubules.

Q, R Quantitative analysis of the incidence of monopolar spindles during the first (Q) and second (R) meiotic divisions for each experimental condition. Percentage of monopolar spindle functional analysis is represented for 100 μM BI2536 and 10 μM MLN8237 for 8-h treatments on organotypic cultures of seminiferous tubules. Experiments were conducted in three different biological replicates. Bars and error bars indicate mean ± SD; *$P < 0.05$, **$P < 0.01$, ***$P < 0.001$, Student's *t*-test.

Data information: White arrows indicate the location of centrosomes. Scale bar in P represents 10 μm.
Source data are available online for this figure.

bipolar and monopolar spindles I and II (Fig 8C and D). AURKP signal intensity at poles is statistically reduced in monopolar spindles of *Plk1*(Δ/Δ), BI2536-treated and MLN8237-treated spermatocytes against control (Fig 8E). Intensity quantification of AURKP at the poles in metaphases II and monopolar spindles II was not conducted since the chromosome configuration as a compact crown very near to the poles could interfere with the signal measurement.

Altogether, these results suggest that the depletion of *Plk1* or inhibition of PLK1 impairs the phosphorylation of centrosomal AURK in monopolar spindles I and II. In addition, it suggests that AURKA could have an autophosphorylating capacity in meiotic centrosomes.

PLK1 plays a role in CEP250 disruption at the onset of centrosome migration and in regulating KIF11 to establish bipolar spindles during male mouse meiosis

We finally studied CEP250, a component of the proteinaceous link that joins paternal centrioles from preduplication and holds them together until centrosome separation in late G2 (Mayor *et al*, 2000). We wondered if CEP250 showed any alterations in the experimental conditions studied. Our data suggest that CEP250 is detected at the centrosomes until late diplotene in control individuals, where it disappeared with the onset of centrosome migration (Fig 9A a). No signal of CEP250 persisted at control metaphase I (Fig 9A b). In contrast, when centrosome migration was arrested in *Plk1*(Δ/Δ) diplotenes, the CEP250 link remains visible between non-migrated centrosomes until metaphases I in monopolar spindles I (Fig 9A c and d).

Assuming that *Plk1*(Δ/Δ) adjacent centrosomes in diakinesis would not be able to recruit KIF11, we then immunolabelled this kinesin in monopolar spindles. While control spermatocytes showed KIF11 decorating the spindle structure of control bipolar spindles (Fig 9B a), spermatocytes under *Plk1* depletion -*Plk1*(Δ/Δ)- or PLK1 inhibition -BI2536-, and also after AURKA inhibition -MLN8237-, showed an impairment of KIF11 localisation to monopolar spindles (Fig 9B b–d). These results indicate that KIF11 is a downstream effector of PLK1/AURKA cascade to establish the bipolar spindles during meiosis and offers a mechanistical explanation for the generation of monopolar spindles after PLK1 alteration.

Discussion

Centrosome and spindle dynamics in male mouse meiosis

Meiosis, in contrast to mitosis, involves two consecutive rounds of cell division. This inevitably requires a strict regulation of centrosomes to ensure the formation of efficient gametes.

We confirmed the presence of CETN3, PCNT and γ-Tubulin in meiotic centrosomes throughout the two meiotic divisions, suggesting a similar composition to mitotic centrosomes (Middendorp *et al*, 1997; Woodruff *et al*, 2014). Our data suggest that centrosome duplication occurs twice during male mouse meiosis. First centrosome duplication occurs once meiosis has started, in the transition from leptotene to zygotene, in contrast to mitotic centrosome duplication in premitotic S phase (Arbi *et al*, 2018). Second centrosome duplication occurs in interkinesis, similarly to previous results described for *C. elegans* (Peters *et al*, 2010). This dual centrosome duplication in male mouse meiosis allows the formation of four spermatids per each spermatogonia that enters meiosis, each one with two centrioles (Manandhar *et al*, 2005).

Somatic cell centrosomes undergo a maturation process that occurs at the end of G2, before the entry into mitosis (Conduit *et al*, 2015). Our results indicate that the complete maturation of meiotic centrosomes occurs throughout prophase I and prophase II stages, as changes in PCM components as PCNT were appreciated till late prophase I and II. In mitosis, this maturation process is related to the dissolution of a proteinaceous link containing CEP250 that binds the two parental centrioles, which occurs before entry to mitosis (Mayor *et al*, 2000; Faragher & Fry, 2003). No significant signals of CEP250 could be detected in spermatocytes after diplotene, assuming that this link cleavage must occur immediately before the onset of centrosome migration, from diplotene onwards.

Achieving a functioning male meiosis division as a global process implies the accuracy of several processes. One of the most critical is the establishment of meiotic bipolar spindles. Therefore, in congruence with a dual centrosome duplication during male mouse meiosis, duplicated centrosomes also have to separate twice to ensure the formation of meiotic bipolar spindles I and II. Our data suggest that centrosome migration start at late diplotene, for the first meiotic division. This seems to be preceded by CEP250 disruption. In both

cases, migration occurs before nuclear envelope breaks down (NEBD). For spermatocytes, having separated centrosomes at the time of NEBD could be advantageous as bipolar spindle would be assembled rapidly and MTs can easily capture kinetochores, sharing the model proposed for mitosis (Hames *et al*, 2001; Beaudouin *et al*, 2002). The disorganisation of NE components in this stage is

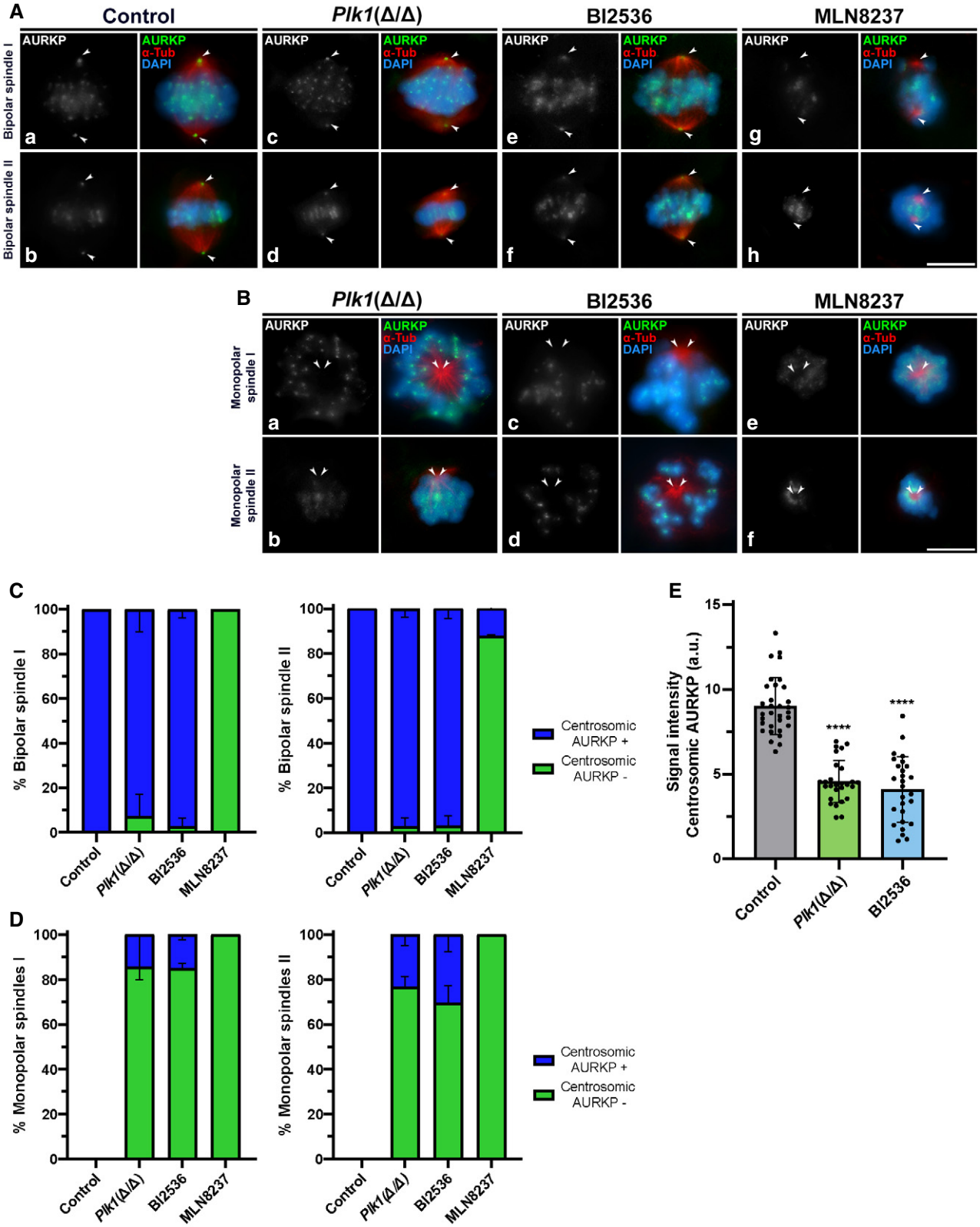

Figure 8.

Figure 8. Analysis of AURKAP in control, *Plk1*(Δ/Δ), BI2536-treated and MLN8237-treated spermatocytes.

A, B AURKP distribution in control, *Plk1*(Δ/Δ), 100 μM 8-h BI2536-treated and 10 μM 8-h MLN8237-treated spermatocytes. (A) Double immunolabelling of AURKP (grey/green) and α-Tubulin (red) in control, *Plk1*(Δ/Δ), BI2536-treated and MLN8237-treated spermatocytes. Images are shown for bipolar spindles I and II for each condition. (B) Monopolar spindles I and II are shown for *Plk1*(Δ/Δ), BI2536-treated and MLN8237-treated spermatocytes. Chromatin has been stained with DAPI (blue).

C Quantification of the percentage of bipolar spindles during the first and second meiotic divisions presenting (blue bars) or lacking (green bars) centrosomic AURKP signals for each experimental condition. Percentage of monopolar spindles is represented for 100 μM BI2536 and 10 μM MLN8237 for 8-h treatments on organotypic cultures of seminiferous tubules. Data represent the average of two biological replicates per condition. Data are mean ± SD.

D Quantification of the percentage of monopolar spindles during the first and second meiotic division presenting (blue bars) or lacking (green bars) centrosomic AURKP signal for each experimental condition. Percentage of monopolar spindles is represented for 100 μM BI2536 and 10 μM MLN8237 for 8-h treatments on organotypic cultures of seminiferous tubules. Data represent the average of two biological replicates per condition. Data are mean ± SD.

E Quantitative analysis of AURKP signal at cell poles. Experiments were conducted for two biological replicates. Number of cells analysed: control (n = 32), *Plk1*(Δ/Δ) (n = 27), BI2536-treated spermatocytes (n = 27). Data are mean ± SD; ****P < 0.0001, Student's t-test.

Data information: White arrows indicate the location of centrosomes. Scale bars in A-h and B-f represent 10 μm.
Source data are available online for this figure.

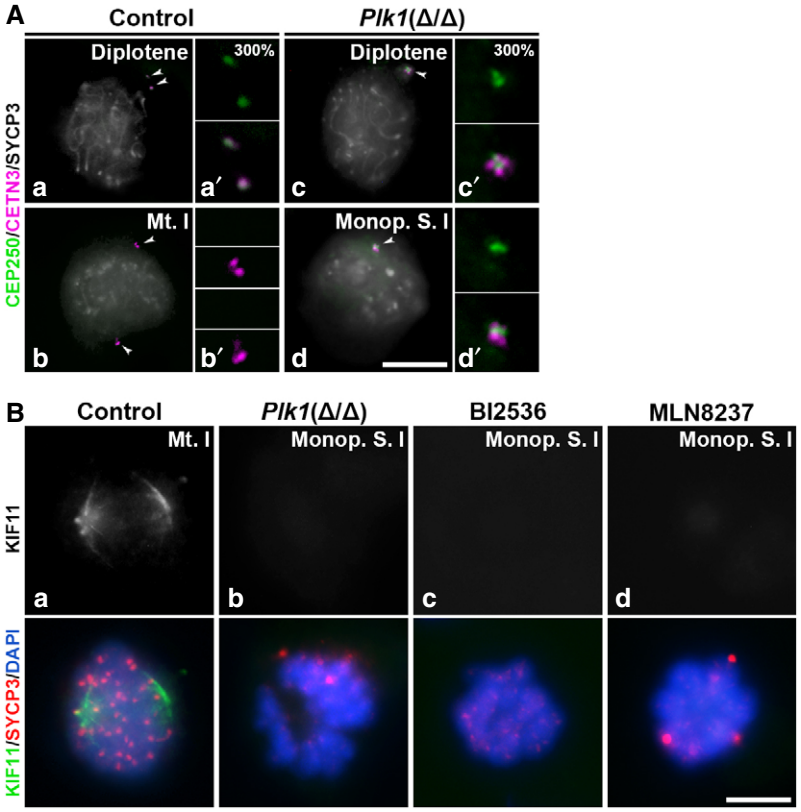

Figure 9. Distribution of CEP250, CETN3 and SYCP3 in control and *Plk1*(Δ/Δ) spermatocytes.

A Triple immunolabelling of CEP250 (green), CETN3 (magenta) and SYCP3 (grey) in (a, b) late diplotene and (c, d) metaphase I in control and *Plk1*(Δ/Δ) spermatocytes.

B Double immunolabelling of KIF11 (grey/green) and SYCP3 (red) in (a) control spindle, (b) *Plk1*(Δ/Δ) monopolar spindle, (c) BI2536 monopolar spindle and (d) MLN8237 monopolar spindle. Chromatin has been stained with DAPI (blue). Data are presented for 100 μM BI2536 and 10 μM MLN8237 for 8-h treatments on organotypic cultures of seminiferous tubules.

Data information: White arrows in A indicate the location of centrosomes. Insets in A correspond to centrosomes at 300% magnification. Scale bar in A-d and B-d represents 10 μm.

presumably coincident with centrosome migration towards the opposite poles, as the formation of the bipolar spindle takes place during the transition from diakinesis to metaphase I. During the second meiotic division, duplicated centrosomes start migrating in late interkinesis, continue their separation in prophase II, and finally form a bipolar spindle in metaphase II.

At metaphase I and II, bipolar spindles I and II, respectively, are established, ensuring chromosome congression at the metaphase plate and the later chromosome segregation at anaphases I and II. During the mitotic cycle, PCM starts disorganising at telophase in a process mediated by PLK1 and Separase (Lee & Rhee, 2012; Matsuo *et al*, 2012), in a presumably similar manner that we observe for

telophase I, where a mild fragmentation of PCNT signals is seen. In contrast, we do not observe a PCNT fragmentation at telophase II. This difference could be explained because somatic cells and telophase I spermatocytes are ready to undergo another cell division, meaning another cell cycle, or the second meiotic division, respectively. Telophase I PCM might need to prepare for the reduplication of centrosomes in interkinesis, while telophase II spermatocytes will continue their development with spermiogenesis, a process that implies their transformation into spermatids and later into mature spermatozoids (Lindemann & Lesich, 2016). The formation of a flagella implies the maturation of the pair of centrioles per spermatid, one of the centrioles is transformed into the axoneme, and finally both distal and proximal centrioles are lost in mature mouse spermatozoa (Manandhar *et al*, 2005; Diniz *et al*, 2012). This important process might need a robust PCM in telophase II in preparation for spermiogenesis. PCNT has been detected at the acrosome region and flagellum neck and middle piece in mouse elongated spermatids (Chang *et al*, 2010), and is later told to disappear during later stages of maturation (Goto & Eddy, 2004; Manandhar *et al*, 2005).

PLK1 role in mouse meiotic centrosome regulation

Although the involvement of PLK1 in mitotic centrosome regulation has been extensively studied (Archambault & Glover, 2009; de Carcer *et al*, 2011; Schmucker & Sumara, 2014; Zitouni *et al*, 2014; Vaid *et al*, 2016), yet not as deeply in relation to the acentriolar mouse oocyte spindle (Wianny *et al*, 1998; Tong *et al*, 2002; Xiong *et al*, 2008; Du *et al*, 2015). In mitosis, the importance of PLK1 kinase activity has been demonstrated by identifying up to 358 centrosomal substrates (Santamaria *et al*, 2011). However, the precise mechanisms underlying the dynamics of male mouse meiotic centrosome regulation are mostly unknown. This work partly elucidates these gaps.

In mitosis, the location, activation and function of PLK1 are greatly regulated, since defects may be involved in the appearance of aneuploidies and tumorigenesis (Liu *et al*, 2017). Residues S137 and T210 are located in the activation loop, and their phosphorylation is essential for the regulation of PLK1 (Tsvetkov & Stern, 2005). Our immunolabelling experiments described PLK1S137P at the centrosomes. PLK1S137P and PLK1T210P were detected in the nucleoplasm and at the chromocentres. This nuclear localisation in prophase I has been previously described, proposing a crucial role of PLK1 in the disassembly of the SC (Jordan *et al*, 2012). In addition, the centrosomic localisation of PLK1S137P throughout the complete meiosis suggests that this kinase may as well play a key role in centrosome regulation in male meiosis, as occurs in mouse oocytes (Du *et al*, 2015).

To elucidate the function of PLK1 on meiotic centrosomes, we studied the meiotic phenotype of *Plk1*(Δ/Δ) (Wachowicz *et al*, 2016; de Carcer *et al*, 2017). This model raised interesting results suggesting a pivotal role of PLK1 on PCM assembly, centrosome migration and bipolar spindle establishment.

PLK1 in meiotic PCM assembly

Pericentrin is the major structural protein of mitotic PMC and is essential for the anchoring of many other centrosome proteins (Delaval & Doxsey, 2010). In somatic cells, PCNT is massively recruited to the centrosome during G2, which makes it possible to anchor γTuRC (Zimmerman *et al*, 2004). The absence of PCNT was significantly detected in *Plk1*(Δ/Δ) early prophase I stages, pointing to an essential role of PLK1 in the recruitment of structural components to the PCM.

Given that an A1 spermatogonia takes approximately 17 days to progress into pachytene (Griswold, 2016), our results suggest that *Plk1*(Δ/Δ) spermatocytes already coursing meiosis at the beginning of the TX treatment had a prior synthesis of highly stable PCM that would allow them to progress normally throughout centrosome maturation. In contrast, *Plk1*(Δ/Δ) premeiotic cells (spermatogonia) entering meiosis as preleptotene under the TX treatment were unable to recruit PCNT to the PCM. Therefore, we suggest that the assembly of meiotic PCM starts in premeiotic stages, similar to the G2 centrosome maturation before the entry into mitosis, where PLK1 performs phosphorylation of PCNT allowing the orderly positioning of this protein in PCM (Lee & Rhee, 2011). Interestingly, centrosome duplication is not altered in early prophase I stages of *Plk1*(Δ/Δ), even when PCM loading to centrosomes has been impeded. This points to different regulators of this process. PLK4 has been appointed to be responsible for centrosome duplication in mitosis (Kleylein-Sohn *et al*, 2007) and might serve the same role in meiosis.

Plk1(Δ/Δ) results regarding PCNT recruitment were not confirmed through *in vitro* inhibition of PLK1 activity with short treatments of BI2536 (Steegmaier *et al*, 2007). Although the organotypic culture of seminiferous tubules allows us to design interesting *in vitro* experiments, long treatments are not possible because the culture itself of seminiferous tubules in the control situation induces the appearance of high levels of apoptosis after 24 h. Taking into account that early prophase I in male meiosis lasts for more than a week (Griswold, 2016; Romer *et al*, 2018; Enguita-Marruedo *et al*, 2019), we would need long treatments of BI2536 on cultured spermatocytes to address an effect of PLK1 inhibition from premeiotic stages to leptotene. Consequently, a 7 days of TX treatment in *Plk1*(Δ/Δ) is long enough to induce a phenotype in early prophase I, where a lack of PCNT is due to the entry into meiosis in the absence of PLK1 kinase activity, arresting a proper maturation of the PCM. In contrast, BI2536 8-h treatment is not long enough to reveal a phenotype in prophase I, although it showed mild PCNT morphological alterations.

We observed a partial co-localisation of PLK1S137P and γ-Tubulin in control prophases I and II, pointing at a structural and functional cooperation similar to mitosis (Dictenberg *et al*, 1998; Haren *et al*, 2009). *Plk1*(Δ/Δ) data suggest that the presence of a robust PCM (PCNT) is essential for the location of γTuRC at meiotic centrosomes, also in accordance with mitosis studies (Haren *et al*, 2009). In summary, the absence of PCNT in *Plk1*(Δ/Δ) and altered PCNT in BI2536 clearly points to a predominant role of PLK1 in the recruitment and maintenance of PCM components.

Altogether, this work proposes a central role of PLK1 in the recruitment and maintenance of PCM and γTuRC, regulating the maturation and stability of the meiotic centrosomes and later facilitating their migration towards opposite poles.

PLK1 and AURAK regulate the establishment of the meiotic bipolar spindles

Our results show that PLK1S137P is detected at the centrosomes of meiotic spindles in mouse spermatocytes. This localisation of PLK1

points out a potential role in regulating the meiotic spindle dynamics, as it occurs in mitosis. In somatic cells, PLK1 activity is required for spindle bipolarity establishment (Sumara *et al*, 2004) and for the initiation of cytokinesis (Brennan *et al*, 2007; Santamaria *et al*, 2011). PLK1-deficient somatic cells fail to form a bipolar mitotic spindle because they are unable to separate their centrosomes (Hanisch *et al*, 2006).

Interestingly, depletion or inhibition of PLK1 arrests centrosome migration in diplotene/diakinesis of *Plk1*(Δ/Δ) and BI2536, but PCNT and γ-Tubulin are not altered at non-migrated centrosomes. This reinforces our hypothesis that PLK1 acts several times during meiosis, one of them specifically in diplotene. This implies that diplotene centrosomes with PCNT and γ-Tubulin, presumably forming a complex, that progress under PLK1 inhibition will not be able to separate, regardless of their well-structured preloaded PCM components.

Results extracted from the model *Plk1*(Δ/Δ) suggest that PLK1 could be prompting the establishment of bipolar spindles in the transitions from diakinesis to metaphase I and from prophase I to metaphase II. The *in vitro* experiments with BI2536 corroborate this hypothesis, since PLK1 inhibition induced an arrest in centrosome migration in late diplotene leading to the formation of monopolar spindles. In two very elegant studies, similar results using the same drug were obtained in mitotic cells (Lenart *et al*, 2007) and mouse oocytes (Du *et al*, 2015).

AURKA belongs to the Aurora kinase family, which plays important roles in the regulation of the centrosome cycle (Nigg & Holland, 2018). These kinases are involved in tumorigenesis processes and are a target for cancer treatment (Kollareddy *et al*, 2012; Tang *et al*, 2017). In particular, AURKAP localises at spindle poles and is involved in the maturation of the centrosome and the establishment of the mitotic (Fu *et al*, 2007; Nikonova *et al*, 2013; Lim *et al*, 2016) and oocyte (Yao *et al*, 2004) spindles.

Although centrosomes did not migrate when PLK1 function was altered, we observed no defects on PCNT in monopolar spindles, nor was its ability to anchor γ-Tubulin impaired in all the experimental conditions. As we have suggested, PCM loading might occur before the entry into meiosis. Taking into account the duration of prophase I (Griswold, 2016; Romer *et al*, 2018; Enguita-Marruedo *et al*, 2019), *Plk1*(Δ/Δ) and BI2536 monopolar spindles might have preloaded PCNT into centrosomes. Previous data in mitosis reported that PCNT persists at centrosomes in metaphase after BI2536 treatment (Kim *et al*, 2015). On the other hand, we neither observed alterations of PCNT, and presumably γ-Tubulin, in MLN8237 monopolar spindles. In this framework, inhibition of AURKA with MLN8237 does not impair γ-Tubulin localisation at centrosomes in somatic cells (Asteriti *et al*, 2014; Ma *et al*, 2014), neither alters the localisation of PCNT in ciliogenesis studies of VLH human cells (Hasanov *et al*, 2017). Moreover, our results reveal that inhibition of PLK1 or AURKA did not alter the ability of centrosomes to nucleate MTs (detected with α-Tubulin) forming monopolar spindles in meiosis I and meiosis II. Previous inhibition studies of PLK1 with BI2536 carried out on mouse oocytes disclosed an important role of PLK1 in the fragmentation of the centrosome, essential for the further nucleation of MTs and the formation of the bipolar acentriolar meiotic spindle (Clift & Schuh, 2015; Severance & Latham, 2017). However, in females, PLK1 is not essential, since its inhibition only produces a bipolarisation delay and a shorter spindle (Solc *et al*, 2015). The clear differences between the acentriolar spindles of oocytes (Manandhar *et al*, 2005) and the centrosome spindle of spermatocytes might explain a difference in the mouse meiotic spindle dynamics between both sexes. All data considered, we suggest that the absence of PLK1 or AURKA kinase activity induces monopolar spindles with non-migrated centrosomes. Nevertheless, the inability to migrate centrosomes in prometaphase does not alter preloaded PCM location and functions in meiotic spindles.

We hypothesise that PLK1 function is essential for the disassembly of CEP250 link between duplicated centrosomes, accordingly to mitotic cells without PLK1 activity (Mardin *et al*, 2011). Our data suggest that CEP250 link is still connecting adjacent centrosomes under Plk1 depletion -*Plk1*(Δ/Δ)- in monopolar spindles, pointing at meiotic PLK1 cascade as the executor of the separation between parental centrioles. The inability of *Plk1*(Δ/Δ) spermatocytes to eliminate CEP250 link from centrioles may be leading to the migration impairment. To further address the implication of PLK1 and AURKA in centrosome migration towards opposite poles in male mouse meiosis, we have also studied the role of these kinases in promoting kinesin KIF11 activity, following the proposed model for mitotic PLK1 (Bertran *et al*, 2011; Kapitein *et al*, 2005). KIF11 is clearly seen decorating the spindle structure of bipolar spindles in control spermatocytes, as previously reported for mitosis (Cochran *et al*, 2004), suggesting that this kinesin also executes the MT forces to separate poles during meiosis. *Plk1*(Δ/Δ), BI2536-treated and MLN8237-treated monopolar spindles showed an impairment of KIF11 localisation to monopolar spindles. This implies that KIF11 is a downstream effector of PLK1, or PLK1 and AURKA, to promote meiotic bipolar spindles, sharing the mitotic model (Ma *et al*, 2014). Without the force of this kinesin, centrosomes will not be able to reach opposite poles. These data reinforce the overlapping functions of both kinases in the regulation of meiotic spindles and offer a mechanistic explanation of the arrest of monopolar spindles in meiosis.

PLK1 and AURKA crosstalk in male mouse meiosis

It is therefore clear that PLK1 is an essential kinase for the regulation of cell division, but in turn it must also be regulated. In mitosis, kinases CDK1 and AURKA play this role (Fu *et al*, 2007; Lukasiewicz & Lingle, 2009). Our results show that the kinase activity of PLK1 and AURKA are both needed for the accurate formation of meiotic bipolar spindles. Elucidating the individual spatial and temporal actions of PLK1 and AURKA is challenging as these kinases continually change their location and activity throughout mitosis (Bruinsma *et al*, 2015; Joukov & De Nicolo, 2018). Previous data suggested that Bora-AURKA complex phosphorylates PLK1 in order to achieve its activation at the end of the G2 phase and promote entry into mitosis (Seki *et al*, 2008). Therefore, in mitosis, AURKA is upstream to PLK1 in the mitotic spindle cascade regulation path. However, other authors suggested that mitotic PLK1 regulates the maintenance of phosphorylated AURKA in the centrosome by controlling cellular levels of Bora (Chan *et al*, 2008). Different authors claimed that PLK1 functions in the centrosome are essential and are maintained throughout the entire cell division process, keeping a feedback loop that involves PCNT, CEP192 and AURKA proteins, essential for the maintenance of the stability of the PCM (Joukov *et al*, 2014; Joukov & De Nicolo, 2018). More recently,

centrosomal anchoring protein Gravin/AKAP12 has been appointed to be important for duration of mitosis and accumulation of active pools of both PLK1 and AURKA at mitotic centrosomes of zebrafish (Bucko *et al*, 2019).

We observed that depletion of *Plk1* in *Plk1*(Δ/Δ), or PLK1 inhibition with BI2536, induces significant reduction of phosphorylation of AURKA at the centrosomes, specifically in monopolar spindles. The absence or reduced levels of AURKAP revealed a PLK1 involvement in the phosphorylation of AURKA in the meiotic centrosome or in the recruitment of AURKAP to the centrosome through other target proteins of the kinase activity of PLK1. It would also be possible that non-phosphorylated AURKA could be playing its kinase role over PLK1, as occurs in mitosis (Seki *et al*, 2008). Partial inhibition of AURK kinases with high doses of BI2536 cannot be excluded. However, BI2536 results replicate most of the results obtained using the *Plk1* genetic depletion model. In addition, our results regarding MLN8237 treatment showed overlapping roles of PLK1 and AURKA. Likewise, our results also point to an autophosphorylation role of AURKA in male meiosis, since its inhibition with MLN8237 impairs its phosphorylation at centrosomes, independently of the accuracy of centrosome migration. AURKA autophosphorylation capacity has also been reported in mitosis (Willems *et al*, 2018).

Our results suggest that both PLK1 and AURKA have predominant, and potentially overlapping, roles in the formation of meiotic bipolar spindles I and II in spermatogenesis. This could imply a continuous implication of these kinases over the progression of meiosis. Our overall data suggest that PLK1 is needed at least thrice during meiosis: it is needed in early prophase I to ensure PCM maturation, ensuring PCNT and γ-Tubulin recruitment; it is later needed in diplotene for CEP250 disruption to allow centrosome migration; and is needed again in diakinesis and prophase II to continue migration and ensure the formation of the meiotic spindles I and II, respectively, thanks to KIF11 pulling forces towards opposite poles. In addition, we suggest that AURKA is equally needed for the formation of bipolar spindles, pointing again to a joined role of both kinases.

Our work suggests that both kinases are indispensable for the formation and maintenance of bipolar spindles in both meiotic divisions. Determining the exact functional interactions between PLK1 and AURKA would be key to address in further studies about the meiotic spindle and the meiotic chromosome segregation.

Materials and Methods

Materials

Seminiferous tubules from adult C57BL/6 wild-type (WT) male mice and *Plk1* conditional depletion male mice (Wachowicz *et al*, 2016; de Carcer *et al*, 2017) were used for this study. The *Plk1* conditional mice included loxP sequences flanking exon 2 of murine PLK1, generating the PLK1 (lox) locus. To generate a null allele *Plk1*(Δ), *Plk1*(lox/lox) mice were crossed with mice carrying RERT2 allele, which includes a tamoxifen-inducible Cre recombinase ubiquitously expressed under the regulatory sequences of RNA polymerase II. To activate Cre recombinase, tamoxifen citrate salt was added to the mice's diet for 7 days and their testes surgically removed after euthanasia. Oligonucleotides for the *Plk1* cKO genotyping: *EX1a_F (5-ACAGCGACTTTGTATTTGTAGTTTTG-3)* and *IN1b_R (5-CACTTTATGAATCCATTTCCTGTACC-3)* for detecting the wild-type and lox alleles and *IN2_R (5-TTTCAGCTTAGTAAAGAGACA-3)* for the depleted allele. Gene strategy and PCR results are displayed in Fig EV3. All animals were kept at the Animal Facility of the Spanish National Cancer Research Centre (CNIO) or Animal Facility of Faculty of Medicine of Universidad Autónoma de Madrid under specific pathogen-free conditions in accordance with the recommendation of the Federation of European Laboratory Animal Science Associations (FELASA). All animal procedures were approved by local and regional ethics committees (Institutional Animal Care and Use Committee and Ethics Committee for Research and Animal Welfare, Instituto de Salud Carlos III) and performed according to the European Union guidelines.

Organotypic culture of seminiferous tubules and inhibition of PLK1 and AURKA

The culture of seminiferous tubules was performed as previously described (Sato *et al*, 2011). Testes were removed and detunicated, and fragments of seminiferous tubules were cultured for at least 2h in agarose gel half-soaked in MEMα culture medium (Gibco A10490-01) supplemented with KnockOut Serum Replacement (KSR) (Gibco 10828-010) and antibiotics (Penicillin/Streptomycin; Biochrom AG, A2213) at 34°C in an atmosphere with 5% CO_2.

Optimisation of control, BI2536-treated and MLN8237-treated cultured spermatocytes is shown in Fig EV4. The reliability of the organotypic culture of seminiferous tubules was analysed at different timings: 2, 4, 8, 24 and 48 h. Analysis of apoptosis levels showed high levels of lethality after 8 h of control cultures (Fig EV4A–C); therefore, confident experiments were narrowed down to 8 h of control or treatment conditions. To inhibit PLK1, 100 μM BI2536 (Selleck Chemicals, S1109) diluted in 10% DMSO was added to the culture medium, and seminiferous tubules were placed over an agarose gel embedded with BI2536 medium and recovered after 8 h of treatment. To inhibit AURKA, 10 μM of MLN8237 – also called Alisertib – (Selleckchem, S1133) diluted in 10% DMSO was added to the culture medium and seminiferous tubules were also recovered after 8 h of treatment. Controls for each experiment were done with seminiferous tubules cultures with 10% DMSO.

Optimisation of BI2536 and MLN8237 concentrations and timing is shown in Fig EV4. We used the appearance of monopolar spindles as a marker of treatment success, as this phenotype has been described in mitosis and oocytes both for BI2536 (Lenart *et al*, 2007; Steegmaier *et al*, 2007; Jordan *et al*, 2012) and MLN8237 (Kollareddy *et al*, 2012; Nguyen *et al*, 2018). For both drugs, 1 μM showed no effect at 2 h and no relevant effect at 4 h or 8 h. Taking into account that control spermatocytes present high level of apoptosis after 8 h of culture, we narrowed this timing for the treatment of both drugs (Fig EV4D). A concentration of 10 μM showed significant level of monopolar spindles with MLN8237, while 100 μM was discarded for high levels of apoptosis. In contrast, 10 μM and 100 μM concentrations for BI2536 both showed significant levels of monopolar spindles in comparison to control spermatocytes and presented no differences in apoptotic markers. The immunolabelling of the proteins studied in this work was identical both for 10 μM and 100 μM of BI2536. 100 μM BI2536 percentage of monopolar

spindles is lower than 10 μM MNL8237 levels. We concluded that 100 μM was the best choice as it offered a more robust phenotype, meaning that the percentage of monopolar spindles was higher without getting into lethal conditions.

Squashing and spreading of spermatocytes

For immunofluorescence analyses, testes were detunicated and seminiferous tubules processed according to previously described protocols for obtaining squashing (Page *et al*, 1998) or spreading (Peters *et al*, 1997) preparations of spermatocytes. All immunolabellings were performed using a 5% PFA fixation solution, except for CEP250 and KIF11 labelling, that was performed with a methanol post-fixation solution after PFA fixation.

Indirect immunofluorescence

After acquiring either squashed or spread preparations, the slides were rinsed three times for 5 min in PBS and incubated with primary and secondary antibodies diluted in PBS. Slides were counterstained with 10 μg/ml 4′,6-diamidino-2-phenylindole (DAPI) for 3 min, rinsed in PBS for 1 min, mounted with Vectashield (Vector Laboratories) and sealed with nail polish.

Antibodies

Details for primary and secondary antibodies are included in Table EV1.

Apoptosis markers

Cleaved caspase-3 was detected by immunostaining according to the protocols shown above. The percentage of apoptotic cells was calculated counting spermatocytes, excluding Sertoli cells and spermatids. Cell numbers are included in the tables in raw data supplementary material, and graphs in Fig EV4. Caspase-positive spermatocytes were quantified for controls at 8, 24 and 48 h. Quantification of caspase-3-positive spermatocytes for *Plk1*(Δ/Δ) mice and for experimental procedures with BI2536 and MLN8237 was done for 2 h, 4 h and 8 h.

Histology

For histological observation of *Plk1*(Δ/Δ) mice, dissected organs were fixed in 10% buffered formalin (Sigma-Aldrich, St. Louis, MO, USA) and embedded in paraffin wax. After standard washes and dehydration, Paraplast-embedded tissue blocks were cut in 3- to 5-μm-thick sections using a Reichert microtome. Sections were stained with conventional Mallory's trichrome stain.

Cryosections

Testes were dissected and placed and wash briefly in ice-cold PBS and fixed in 4% PFA for 24 h. Testes were then placed in 15% sucrose in PBS until tissue sinks (6–12 h) and then in 30% sucrose in PBS for overnight. Testes were cryosected at 14-μm-thick sections, and DAPI counterstaining was done to reveal nucleus of the cells in the seminiferous epithelium.

Image capture and processing

Immunofluorescence images were collected using an Olympus BX61 microscope equipped with epifluorescence optics, a motorised Z-drive and an Olympus digital camera (DP70 or DP71) controlled by AnalySIS software (Olympus Corporation, Japan, 2003). Figures presenting data obtained in squashed spermatocytes were presented as stacks, processed after obtaining complete Z-projections (30–60 focal planes of each cell). Stacks were analysed and processed using the public domain software ImageJ (National Institute of Health, USA, version v.1.52). Final images were processed with Adobe Photoshop (Adobe Inc., USA, version CS6).

Quantification and statistical analyses

Data are presented as mean ± SD of a minimum of three animals for control, BI2536 and MLN8237 have been used, and a minimum of two *Plk1*(Δ/Δ) mice for each quantification (see supplementary raw data file). All statistical analyses were performed using Prism 8 software (GraphPad Software Inc.). Differences were analysed by two-tailed Student's *t*-test or one-way ANOVA. Values of $P < 0.05$ were considered statistically significant.

Data availability

This study includes no data deposited in external repositories.

Expanded View for this article is available online.

Acknowledgements
This work was supported by funding from Ministerio de Economía, Industria y Competitividad, Gobierno de España (MINECO) (Spain) [grant number BFU2014-53681-P and MEIONET (BFU2015-71786-REDT) to J. A. S. and grant number RTI2018-095582-B-I00 to M. M.]. E. A. was supported by grants "Ayuda para Estudios de Master" and "Ayudas PostMaster" from the Department of Biology of the Universidad Autónoma de Madrid (Spain). JGM received a predoctoral contract from the Ministry of Education of Spain (FPI grants). This work is dedicated to Professor Julio Sánchez Rufas (1956-2020). We express our sincere thanks to Jesús Page and Inés Berenguer for providing laboratory equipment and reagents for this study and for contributing to the discussion of results.

Author contributions
RG, EA and PL-J conceived and designed the experiments. RG, EA, JG-M and PL-J performed the experiments. RG, EA, JG-M, PL-J, MM and JAS analysed the data. RG and EA wrote the paper. All authors revised the manuscript.

Conflict of interest
The authors declare that they have no conflict of interest.

References

Agircan FG, Schiebel E, Mardin BR (2014) Separate to operate: control of centrosome positioning and separation. *Philos Trans R Soc Lond B Biol Sci* 369: 20130461

Arbi M, Pefani DE, Taraviras S, Lygerou Z (2018) Controlling centriole numbers: Geminin family members as master regulators of centriole amplification and multiciliogenesis. *Chromosoma* 127: 151 – 174

Archambault V, Glover DM (2009) Polo-like kinases: conservation and divergence in their functions and regulation. *Nat Rev Mol Cell Biol* 10: 265 – 275

Asteriti IA, Di Cesare E, De Mattia F, Hilsenstein V, Neumann B, Cundari E, Lavia P, Guarguaglini G (2014) The Aurora-A inhibitor MLN8237 affects multiple mitotic processes and induces dose-dependent mitotic abnormalities and aneuploidy. *Oncotarget* 5: 6229 – 6242

Azimzadeh J, Marshall WF (2010) Building the centriole. *Curr Biol* 20: R816 – R825

Barr FA, Sillje HH, Nigg EA (2004) Polo-like kinases and the orchestration of cell division. *Nat Rev Mol Cell Biol* 5: 429 – 440

Beaudouin J, Gerlich D, Daigle N, Eils R, Ellenberg J (2002) Nuclear envelope breakdown proceeds by microtubule-induced tearing of the lamina. *Cell* 108: 83 – 96

Bertran MT, Sdelci S, Regue L, Avruch J, Caelles C, Roig J (2011) Nek9 is a Plk1-activated kinase that controls early centrosome separation through Nek6/7 and Eg5. *EMBO J* 30: 2634 – 2647

Blangy A, Lane HA, d'Herin P, Harper M, Kress M, Nigg EA (1995) Phosphorylation by p34cdc2 regulates spindle association of human Eg5, a kinesin-related motor essential for bipolar spindle formation *in vivo*. *Cell* 83: 1159 – 1169

Bornens M (2012) The centrosome in cells and organisms. *Science* 335: 422 – 426

Brennan IM, Peters U, Kapoor TM, Straight AF (2007) Polo-like kinase controls vertebrate spindle elongation and cytokinesis. *PLoS One* 2: e409

Bruinsma W, Aprelia M, Kool J, Macurek L, Lindqvist A, Medema RH (2015) Spatial separation of Plk1 phosphorylation and activity. *Front Oncol* 5: 132

Bucko PJ, Lombard CK, Rathbun L, Garcia I, Bhat A, Wordeman L, Smith FD, Maly DJ, Hehnly H, Scott JD (2019) Subcellular drug targeting illuminates local kinase action. *Elife* 8: e52220

de Carcer G, Manning G, Malumbres M (2011) From Plk1 to Plk5: functional evolution of polo-like kinases. *Cell Cycle* 10: 2255 – 2262

de Carcer G, Wachowicz P, Martinez-Martinez S, Oller J, Mendez-Barbero N, Escobar B, Gonzalez-Loyola A, Takaki T, El Bakkali A, Camara JA *et al* (2017) Plk1 regulates contraction of postmitotic smooth muscle cells and is required for vascular homeostasis. *Nat Med* 23: 964 – 974

Chan EH, Santamaria A, Sillje HH, Nigg EA (2008) Plk1 regulates mitotic Aurora A function through betaTrCP-dependent degradation of hBora. *Chromosoma* 117: 457 – 469

Chang YC, Chen YJ, Wu CH, Wu YC, Yen TC, Ouyang P (2010) Characterization of centrosomal proteins Cep55 and pericentrin in intercellular bridges of mouse testes. *J Cell Biochem* 109: 1274 – 1285

Clift D, Schuh M (2015) A three-step MTOC fragmentation mechanism facilitates bipolar spindle assembly in mouse oocytes. *Nat Commun* 6: 7217

Cochran JC, Sontag CA, Maliga Z, Kapoor TM, Correia JJ, Gilbert SP (2004) Mechanistic analysis of the mitotic kinesin Eg5. *J Biol Chem* 279: 38861 – 38870

Coelho PA, Bury L, Sharif B, Riparbelli MG, Fu J, Callaini G, Glover DM, Zernicka-Goetz M (2013) Spindle formation in the mouse embryo requires Plk4 in the absence of centrioles. *Dev Cell* 27: 586 – 597

Conduit PT, Wainman A, Raff JW (2015) Centrosome function and assembly in animal cells. *Nat Rev Mol Cell Biol* 16: 611 – 624

Delaval B, Doxsey SJ (2010) Pericentrin in cellular function and disease. *J Cell Biol* 188: 181 – 190

Dictenberg JB, Zimmerman W, Sparks CA, Young A, Vidair C, Zheng Y, Carrington W, Fay FS, Doxsey SJ (1998) Pericentrin and gamma-tubulin form a protein complex and are organized into a novel lattice at the centrosome. *J Cell Biol* 141: 163 – 174

Diniz MC, Pacheco AC, Farias KM, de Oliveira DM (2012) The eukaryotic flagellum makes the day: novel and unforeseen roles uncovered after post-genomics and proteomics data. *Curr Protein Pept Sci* 13: 524 – 546

Du J, Cao Y, Wang Q, Zhang N, Liu X, Chen D, Liu X, Xu Q, Ma W (2015) Unique subcellular distribution of phosphorylated Plk1 (Ser137 and Thr210) in mouse oocytes during meiotic division and pPlk1(Ser137) involvement in spindle formation and REC8 cleavage. *Cell Cycle* 14: 3566 – 3579

Dumont J, Desai A (2012) Acentrosomal spindle assembly and chromosome segregation during oocyte meiosis. *Trends Cell Biol* 22: 241 – 249

Enguita-Marruedo A, Martin-Ruiz M, Garcia E, Gil-Fernandez A, Parra MT, Viera A, Rufas JS, Page J (2019) Transition from a meiotic to a somatic-like DNA damage response during the pachytene stage in mouse meiosis. *PLoS Genet* 15: e1007439

Fabbro M, Zhou BB, Takahashi M, Sarcevic B, Lal P, Graham ME, Gabrielli BG, Robinson PJ, Nigg EA, Ono Y *et al* (2005) Cdk1/Erk2- and Plk1-dependent phosphorylation of a centrosome protein, Cep55, is required for its recruitment to midbody and cytokinesis. *Dev Cell* 9: 477 – 488

Faragher AJ, Fry AM (2003) Nek2A kinase stimulates centrosome disjunction and is required for formation of bipolar mitotic spindles. *Mol Biol Cell* 14: 2876 – 2889

Fu J, Bian M, Jiang Q, Zhang C (2007) Roles of Aurora kinases in mitosis and tumorigenesis. *Mol Cancer Res* 5: 1 – 10

Fujita H, Yoshino Y, Chiba N (2016) Regulation of the centrosome cycle. *Mol Cell Oncol* 3: e1075643

Goto M, Eddy EM (2004) Speriolin is a novel spermatogenic cell-specific centrosomal protein associated with the seventh WD motif of Cdc20. *J Biol Chem* 279: 42128 – 42138

Griswold MD (2016) Spermatogenesis: The Commitment to Meiosis. *Physiol Rev* 96: 1 – 17

Hames RS, Wattam SL, Yamano H, Bacchieri R, Fry AM (2001) APC/C-mediated destruction of the centrosomal kinase Nek2A occurs in early mitosis and depends upon a cyclin A-type D-box. *EMBO J* 20: 7117 – 7127

Hanisch A, Wehner A, Nigg EA, Sillje HH (2006) Different Plk1 functions show distinct dependencies on Polo-Box domain-mediated targeting. *Mol Biol Cell* 17: 448 – 459

Haren L, Remy MH, Bazin I, Callebaut I, Wright M, Merdes A (2006) NEDD1-dependent recruitment of the gamma-tubulin ring complex to the centrosome is necessary for centriole duplication and spindle assembly. *J Cell Biol* 172: 505 – 515

Haren L, Stearns T, Luders J (2009) Plk1-dependent recruitment of gamma-tubulin complexes to mitotic centrosomes involves multiple PCM components. *PLoS One* 4: e5976

Hasanov E, Chen G, Chowdhury P, Weldon J, Ding Z, Jonasch E, Sen S, Walker CL, Dere R (2017) Ubiquitination and regulation of AURKA identifies a hypoxia-independent E3 ligase activity of VHL. *Oncogene* 36: 3450 – 3463

Hauf S, Roitinger E, Koch B, Dittrich CM, Mechtler K, Peters JM (2005) Dissociation of cohesin from chromosome arms and loss of arm cohesion during early mitosis depends on phosphorylation of SA2. *PLoS Biol* 3: e69

Hunt PA, Hassold TJ (2002) Sex matters in meiosis. *Science* 296: 2181 – 2183

Hunter N (2015) Meiotic recombination: the essence of heredity. *Cold Spring Harb Perspect Biol* 7: a016618

Jordan PW, Karppinen J, Handel MA (2012) Polo-like kinase is required for synaptonemal complex disassembly and phosphorylation in mouse spermatocytes. *J Cell Sci* 125: 5061 – 5072

Joukov V, De Nicolo A (2018) Aurora-PLK1 cascades as key signaling modules in the regulation of mitosis. *Sci Signal* 11: eaar4195

Joukov V, Walter JC, De Nicolo A (2014) The Cep192-organized aurora A-Plk1 cascade is essential for centrosome cycle and bipolar spindle assembly. *Mol Cell* 55: 578 – 591

Kang YH, Park CH, Kim TS, Soung NK, Bang JK, Kim BY, Park JE, Lee KS (2011) Mammalian polo-like kinase 1-dependent regulation of the PBIP1-CENP-Q complex at kinetochores. *J Biol Chem* 286: 19744 – 19757

Kapitein LC, Peterman EJ, Kwok BH, Kim JH, Kapoor TM, Schmidt CF (2005) The bipolar mitotic kinesin Eg5 moves on both microtubules that it crosslinks. *Nature* 435: 114 – 118

Khodjakov A, Rieder CL (2001) Centrosomes enhance the fidelity of cytokinesis in vertebrates and are required for cell cycle progression. *J Cell Biol* 153: 237 – 242

Kim J, Lee K, Rhee K (2015) PLK1 regulation of PCNT cleavage ensures fidelity of centriole separation during mitotic exit. *Nat Commun* 6: 10076

Kleylein-Sohn J, Westendorf J, Le Clech M, Habedanck R, Stierhof YD, Nigg EA (2007) Plk4-induced centriole biogenesis in human cells. *Dev Cell* 13: 190 – 202

Kline-Smith SL, Walczak CE (2004) Mitotic spindle assembly and chromosome segregation: refocusing on microtubule dynamics. *Mol Cell* 15: 317 – 327

Kollareddy M, Zheleva D, Dzubak P, Brahmkshatriya PS, Lepsik M, Hajduch M (2012) Aurora kinase inhibitors: progress towards the clinic. *Invest New Drugs* 30: 2411 – 2432

Lee K, Rhee K (2011) PLK1 phosphorylation of pericentrin initiates centrosome maturation at the onset of mitosis. *J Cell Biol* 195: 1093 – 1101

Lee K, Rhee K (2012) Separase-dependent cleavage of pericentrin B is necessary and sufficient for centriole disengagement during mitosis. *Cell Cycle* 11: 2476 – 2485

Lenart P, Petronczki M, Steegmaier M, Di Fiore B, Lipp JJ, Hoffmann M, Rettig WJ, Kraut N, Peters JM (2007) The small-molecule inhibitor BI 2536 reveals novel insights into mitotic roles of polo-like kinase 1. *Curr Biol* 17: 304 – 315

Lim NR, Yeap YY, Ang CS, Williamson NA, Bogoyevitch MA, Quinn LM, Ng DC (2016) Aurora A phosphorylation of WD40-repeat protein 62 in mitotic spindle regulation. *Cell Cycle* 15: 413 – 424

Lindemann CB, Lesich KA (2016) Functional anatomy of the mammalian sperm flagellum. *Cytoskeleton* 73: 652 – 669

Liu Z, Sun Q, Wang X (2017) PLK1, A Potential Target for Cancer Therapy. *Transl Oncol* 10: 22 – 32

Lukasiewicz KB, Lingle WL (2009) Aurora A, centrosome structure, and the centrosome cycle. *Environ Mol Mutagen* 50: 602 – 619

Ma HT, Erdal S, Huang S, Poon RY (2014) Synergism between inhibitors of Aurora A and KIF11 overcomes KIF15-dependent drug resistance. *Mol Oncol* 8: 1404 – 1418

Manandhar G, Schatten H, Sutovsky P (2005) Centrosome reduction during gametogenesis and its significance. *Biol Reprod* 72: 2 – 13

Mardin BR, Agircan FG, Lange C, Schiebel E (2011) Plk1 controls the Nek2A-PP1gamma antagonism in centrosome disjunction. *Curr Biol* 21: 1145 – 1151

Matsuo K, Ohsumi K, Iwabuchi M, Kawamata T, Ono Y, Takahashi M (2012) Kendrin is a novel substrate for separase involved in the licensing of centriole duplication. *Curr Biol* 22: 915 – 921

Mayor T, Stierhof YD, Tanaka K, Fry AM, Nigg EA (2000) The centrosomal protein C-Nap1 is required for cell cycle-regulated centrosome cohesion. *J Cell Biol* 151: 837 – 846

Middendorp S, Paoletti A, Schiebel E, Bornens M (1997) Identification of a new mammalian centrin gene, more closely related to Saccharomyces cerevisiae CDC31 gene. *Proc Natl Acad Sci USA* 94: 9141 – 9146

Miller MP, Amon A, Unal E (2013) Meiosis I: when chromosomes undergo extreme makeover. *Curr Opin Cell Biol* 25: 687 – 696

Nguyen AL, Drutovic D, Vazquez BN, El Yakoubi W, Gentilello AS, Malumbres M, Solc P, Schindler K (2018) Genetic Interactions between the Aurora Kinases Reveal New Requirements for AURKB and AURKC during Oocyte Meiosis. *Curr Biol* 28: e3455

Nguyen AL, Schindler K (2017) Specialize and divide (Twice): functions of three aurora kinase homologs in mammalian oocyte meiotic maturation. *Trends Genet* 33: 349 – 363

Nigg EA, Holland AJ (2018) Once and only once: mechanisms of centriole duplication and their deregulation in disease. *Nat Rev Mol Cell Biol* 19: 297 – 312

Nikonova AS, Astsaturov I, Serebriiskii IG, Dunbrack Jr RL, Golemis EA (2013) Aurora A kinase (AURKA) in normal and pathological cell division. *Cell Mol Life Sci* 70: 661 – 687

Page J, Suja JA, Santos JL, Rufas JS (1998) Squash procedure for protein immunolocalization in meiotic cells. *Chromosome Res* 6: 639 – 642

Page SL, Hawley RS (2004) The genetics and molecular biology of the synaptonemal complex. *Annu Rev Cell Dev Biol* 20: 525 – 558

Parra MT, Viera A, Gomez R, Page J, Benavente R, Santos JL, Rufas JS, Suja JA (2004) Involvement of the cohesin Rad21 and SCP3 in monopolar attachment of sister kinetochores during mouse meiosis I. *J Cell Sci* 117: 1221 – 1234

Peters AH, Plug AW, van Vugt MJ, de Boer P (1997) A drying-down technique for the spreading of mammalian meiocytes from the male and female germline. *Chromosome Res* 5: 66 – 68

Peters N, Perez DE, Song MH, Liu Y, Muller-Reichert T, Caron C, Kemphues KJ, O'Connell KF (2010) Control of mitotic and meiotic centriole duplication by the Plk4-related kinase ZYG-1. *J Cell Sci* 123: 795 – 805

Piel M, Nordberg J, Euteneuer U, Bornens M (2001) Centrosome-dependent exit of cytokinesis in animal cells. *Science* 291: 1550 – 1553

Romer KA, de Rooij DG, Kojima ML, Page DC (2018) Isolating mitotic and meiotic germ cells from male mice by developmental synchronization, staging, and sorting. *Dev Biol* 443: 19 – 34

Santamaria A, Wang B, Elowe S, Malik R, Zhang F, Bauer M, Schmidt A, Sillje HH, Korner R, Nigg EA (2011) The Plk1-dependent phosphoproteome of the early mitotic spindle. *Mol Cell Proteomics* 10: M110.004457

Saskova A, Solc P, Baran V, Kubelka M, Schultz RM, Motlik J (2008) Aurora kinase A controls meiosis I progression in mouse oocytes. *Cell Cycle* 7: 2368 – 2376

Sato T, Katagiri K, Yokonishi T, Kubota Y, Inoue K, Ogonuki N, Matoba S, Ogura A, Ogawa T (2011) *In vitro* production of fertile sperm from murine spermatogonial stem cell lines. *Nat Commun* 2: 472

Schmucker S, Sumara I (2014) Molecular dynamics of PLK1 during mitosis. *Mol Cell Oncol* 1: e954507

Seki A, Coppinger JA, Jang CY, Yates JR, Fang G (2008) Bora and the kinase Aurora a cooperatively activate the kinase Plk1 and control mitotic entry. *Science* 320: 1655 – 1658

Severance AL, Latham KE (2017) PLK1 regulates spindle association of phosphorylated eukaryotic translation initiation factor 4E-binding protein and spindle function in mouse oocytes. *Am J Physiol Cell Physiol* 313: C501 – C515

Sluder G (2014) One to only two: a short history of the centrosome and its duplication. *Philos Trans R Soc Lond B Biol Sci* 369: 20130455

Solc P, Kitajima TS, Yoshida S, Brzakova A, Kaido M, Baran V, Mayer A, Samalova P, Motlik J, Ellenberg J (2015) Multiple requirements of PLK1 during mouse oocyte maturation. *PLoS One* 10: e0116783

Steegmaier M, Hoffmann M, Baum A, Lenart P, Petronczki M, Krssak M, Gurtler U, Garin-Chesa P, Lieb S, Quant J *et al* (2007) BI 2536, a potent and selective inhibitor of polo-like kinase 1, inhibits tumor growth *in vivo*. *Curr Biol* 17: 316 – 322

Steffen W, Fuge H, Dietz R, Bastmeyer M, Muller G (1986) Aster-free spindle poles in insect spermatocytes: evidence for chromosome-induced spindle formation? *J Cell Biol* 102: 1679 – 1687

Sumara I, Gimenez-Abian JF, Gerlich D, Hirota T, Kraft C, de la Torre C, Ellenberg J, Peters JM (2004) Roles of polo-like kinase 1 in the assembly of functional mitotic spindles. *Curr Biol* 14: 1712 – 1722

Sunkel CE, Glover DM (1988) polo, a mitotic mutant of Drosophila displaying abnormal spindle poles. *J Cell Sci* 89(Pt 1): 25 – 38

Tang A, Gao K, Chu L, Zhang R, Yang J, Zheng J (2017) Aurora kinases: novel therapy targets in cancers. *Oncotarget* 8: 23937 – 23954

Tong C, Fan HY, Lian L, Li SW, Chen DY, Schatten H, Sun QY (2002) Polo-like kinase-1 is a pivotal regulator of microtubule assembly during mouse oocyte meiotic maturation, fertilization, and early embryonic mitosis. *Biol Reprod* 67: 546 – 554

Tsvetkov L, Stern DF (2005) Phosphorylation of Plk1 at S137 and T210 is inhibited in response to DNA damage. *Cell Cycle* 4: 166 – 171

Vaid R, Sharma N, Chauhan S, Deshta A, Dev K, Sourirajan A (2016) Functions of polo-like kinases: a journey from yeast to humans. *Protein Pept Lett* 23: 185 – 197

Wachowicz P, Fernandez-Miranda G, Marugan C, Escobar B, de Carcer G (2016) Genetic depletion of Polo-like kinase 1 leads to embryonic lethality due to mitotic aberrancies. *BioEssays* 38(Suppl 1): S96 – S106

Wianny F, Tavares A, Evans MJ, Glover DM, Zernicka-Goetz M (1998) Mouse polo-like kinase 1 associates with the acentriolar spindle poles, meiotic chromosomes and spindle midzone during oocyte maturation. *Chromosoma* 107: 430 – 439

Willems E, Dedobbeleer M, Digregorio M, Lombard A, Lumapat PN, Rogister B (2018) The functional diversity of Aurora kinases: a comprehensive review. *Cell Div* 13: 7

Woodruff JB, Wueseke O, Hyman AA (2014) Pericentriolar material structure and dynamics. *Philos Trans R Soc Lond B Biol Sci* 369: 20130459

Xiong B, Sun SC, Lin SL, Li M, Xu BZ, OuYang YC, Hou Y, Chen DY, Sun QY (2008) Involvement of Polo-like kinase 1 in MEK1/2-regulated spindle formation during mouse oocyte meiosis. *Cell Cycle* 7: 1804 – 1809

Yao J, Fu C, Ding X, Guo Z, Zenreski A, Chen Y, Ahmed K, Liao J, Dou Z, Yao X (2004) Nek2A kinase regulates the localization of numatrin to centrosome in mitosis. *FEBS Lett* 575: 112 – 118

Zheng Y, Wong ML, Alberts B, Mitchison T (1995) Nucleation of microtubule assembly by a gamma-tubulin-containing ring complex. *Nature* 378: 578 – 583

Zimmerman WC, Sillibourne J, Rosa J, Doxsey SJ (2004) Mitosis-specific anchoring of gamma tubulin complexes by pericentrin controls spindle organization and mitotic entry. *Mol Biol Cell* 15: 3642 – 3657

Zitouni S, Nabais C, Jana SC, Guerrero A, Bettencourt-Dias M (2014) Polo-like kinases: structural variations lead to multiple functions. *Nat Rev Mol Cell Biol* 15: 433 – 452